

NASA CR71115

VISCOUS AND VISCOELASTIC BEHAVIOR OF
1,3,5-tri- α -NAPHTHYL BENZENE

GPO PRICE \$ _____

CFSTI PRICE(S) \$ _____

Hard copy (HC) 3.00

Microfiche (MF) .65

ff 653 July 65

Donald J. Plazek

and

Joseph H. Magill

Mellon Institute
Pittsburgh, Pennsylvania

FACILITY FORM 602

N67-17772

(ACCESSION NUMBER)

66

(PAGES)

CR 71115

(NASA CR OR TMX OR AD NUMBER)

(THRU)

1

(CODE)

06

(CATEGORY)

Presented in part at the 34th Annual Meeting of Society of Rheology
at Mellon Institute, Pittsburgh, Pennsylvania, October 26-29, 1964.

N67-17772

ABSTRACT

The torsional creep and creep recovery behavior of amorphous 1,3,5-tri- α -naphthyl benzene was studied; while at metastable equilibrium density; along a specified glassy volume-temperature line; and during isothermal volume contraction below the conventional glass transition temperature; T_g . Dilatometric measurements confirmed the conventional T_g to be 69°C. The capillary viscosity measurements of Magill and Ubbelohde were extended from 185°C to below T_g , covering viscosity values from 10^{-1} to 10^{16} Poises. In a region of time scale the mechanical response was found to be dominated by Andrade creep. The retardation spectrum found was over 9 logarithmic decades wide in contrast to reportedly narrow spectra exhibited by other liquids with similar molecular weights. A steady state compliance, J_e , of 2.6×10^{-10} cm²/dyne at 64.2°C was measured. Free volume theory was found applicable to all measurements made below 120°C. The occupied volume, v_o , was deduced to be temperature insensitive.

Author



INTRODUCTION

The viscoelastic behavior of polar, low molecular weight ($< 10^3$) organic liquids has been the object of several investigations which utilized dynamic mechanical techniques.¹⁻⁶ For liquids of low viscosity, relaxation phenomena are observed at high frequencies ($< 10^6$ cycles/sec), but for super-cooled liquids where high viscosities are encountered, relaxation effects occur and can be measured at low audio and subaudio frequencies. Close to or below the glass transition temperature, T_g , of a super-cooled liquid, time dependent mechanical response can be observed in the region of time scale conveniently accessible in creep and stress relaxation measurements. Ball indentation creep measurements have been made by Tobolsky and Taylor⁷ on an organic glass-forming material, Galex.

The results of torsional creep and recovery measurements on a highly purified sample of 1,3,5-tri- α -naphthyl benzene, TONB, are reported here. Molecular models of this non-polar compound are non-planar; the naphthalene groups are sterically hindered from lying in the plane of the benzene ring (see schematic drawing). X-ray measurements suggest that the naphthalene planes are at large angles to the benzene plane in the crystal. Since the naphthalene groups presumably cannot rotate, two steric isomers should exist but thin-layer chromatography indicates that only one species is present. In addition, limited x-ray measurements indicate the existence of only one crystalline habit.⁸

Dilatometric measurements of the volume temperature dependence between 25° and 310° of TαNB were made by Magill and Ubbelohde⁹ along with vapor pressure (430-530°C) and capillary viscosity measurements (185-310°C). The dilatometric measurements showed that it was possible to move conveniently along either the crystal or super-cooled liquid branches of the phase diagram. Measurements of the viscous and visco-elastic response of TαNB are of interest as a rare example of a low molecular weight, non-polar glass-former. In addition, these results allow a direct check of the influence of the melt viscosity on the crystal growth rate. This relationship is the subject of a companion paper which follows this description of the creep and recovery behavior of super-cooled liquid and of glassy TαNB.

Materials

1:3:5 tri- α -naphthylbenzene was prepared from 1' acetonaphthone using a procedure similar to that described in the literature.^{10,11} The condensation reaction was conducted in an atmosphere of nitrogen, and the water was azeotroped off during the ten hour heating period. From the solid tarry product, which formed on cooling the contents of the reaction flask, the crude hydrocarbon was isolated using glacial acetic acid and acetic anhydride.

Purification

This crude material was further recrystallized several times from 50/50 chloroform-petroleum ether solutions. The white crystalline needles, obtained at this stage, were further purified by chromatography on Fisher activated alumina (80-200 mesh) using carbon tetrachloride as the eluent. This procedure was repeated three times, after which the solution was passed through a fine sintered glass filter. The hydrocarbon compound was recovered by solvent evaporation, and then recrystallized from toluene. Traces of toluene were removed by heating the TaNB crystals under vacuum (10^{-4} mm Hg pressure) around 100°C.

Dilatometry

Dilatometers were constructed in the conventional manner. The compound (1-1.5 g) was degassed in the dilatometer bulb prior to the addition of pure dry mercury which was used as the indicator liquid.

The dilatometer stem consisted of 1.5 mm diameter precision bore capillary tubing. From the change in volume of the contents of the dilatometer, the density of the ToNB was calculated by the usual procedures after the dilatometer volume was determined with mercury alone.

Creep Apparatus and Sample Handling

The torsional creep apparatus utilized in this investigation consists of a rotor which is magnetically levitated in a controlled atmosphere chamber by means of a solenoid. The current in this solenoid is regulated with an electronic feedback circuit that was designed by Dr. Victor MacCosham.¹² Constant torques were induced in the rotor by means of a drag cup motor and angles reflecting the torsional deformation in the cylindrical samples were monitored with a light lever and a Beckman Photopen recorder. Experimental temperatures were held constant to within 0.05°C with a silicone oil bath (Dow Corning 550).

Pellets of the ToNB were molded in a vacuum stainless steel mold. A specimen was placed in the instrument on a circular sample surface and melted. A second, matching surface was lowered onto the liquid and the distance between the surfaces was adjusted until the material filled the gap. Surface tension held the liquid in the shape of a cylinder with a height in the neighborhood of 0.15 cm. Sample surfaces of 0.6, 1.2, and 3.0 cm in diameter were employed in this study. Absolute values of the creep compliance were obtained at and above 69°C. For measurements below 69°C, the sample was drawn into a long thin cylinder

in order to maintain total angular deformations of about 2 degrees. Absolute values of compliance were obtained from the relative measurements made on the drawn sample by establishing the sample coefficient with check runs at 69°C. No perceptible strain was observed in these drawn samples when they were examined with a polarizing microscope.

At higher temperatures where the viscosity, η , dynes sec/cm², was less than 10⁴ Poise, the instrument was used as a rotational viscometer.

RESULTS

Creep and Recovery Measurements at Equilibrium Volume

Although the conventional glass temperature, T_g , of TONB (determined dilatometrically with one degree per minute cooling) is 69°C , it is possible to reach the equilibrium volume at 59°C in about 10^5 seconds. Our judgment on this point is guided by isothermal volume contraction measurements, which will be discussed later, and is substantiated by repeated creep measurements. Shown in Fig. 1 are creep compliance, $J(t)$, cm^2/dyne curves obtained after cooling from 70°C and equilibrating the temperature of the sample at 59.2°C . The first measurement was taken about four hours after the attainment of thermal equilibrium. The response of the sample on the second day, some 22 hours after reaching 59°C , had slowed down by a factor of 2.32. From the second to the fifth day, the factor was 1.09.

The recoverable compliance curves, $J_r(t)$, for the three measurements were obtained from the early part of the recovery portions of the runs. They are also plotted in Fig. 1. Within experimental uncertainty, the $J_r(t)$ curves measured on the second and the fifth days are identical. The $J(t)$ curve measured on the fifth day was taken to represent the behavior at the equilibrium density. In the preceding statements, we have implicitly assumed that the changing response was entirely a time-scale shift. Such an assumption is consistent with the shape of the curves and no change in amplitude or shape of the retardation spectrum during isothermal contraction need be invoked. The recovery data shown in Fig. 1 are linear with the cube root of time and have a common extrapolated intercept at zero time.

In Fig. 2 all of the creep compliance curves, $J(t)$, are shown which were measured at equilibrium volume and where a significant amount of recoverable deformation was observed. It is clear from the observed curvature that response is viscoelastic in the region of glassy hardness, 10^{-10} cm²/dynes, but it is not immediately obvious that the behavior is not simply Maxwellian (instantaneous elastic plus viscous deformation); in other words, that the recovery is time independent. In the regions where $\log J(t)$ is a straight line with a slope of one on this logarithmic plot, simple viscous flow is the only measurable contribution to the deformation.

To investigate the recoverable compliance behavior one can subtract off the viscous contribution to the compliance since $J_r(t) = J(t) - t/\eta$, but such subtractions lead to unacceptably large errors where the viscous term, t/η , dominates. Therefore, it is highly desirable to measure the characteristic recoverable compliance directly by means of a recovery measurement following a creep run that has achieved steady-state, i.e., after the recoverable component of the deformation has become independent of the time of creep. The corresponding limiting compliance is the steady-state compliance, J_e . Under conditions where steady-state has not been achieved, $J_r(t)$ is well approximated by the recovery measurement for the times of recovery that are much less than the time of creep.

Recovery measurements made at four temperatures are shown in Fig. 3. These $J_r(t)$ curves describe a surprisingly broad retarded transition. At three of the temperatures, 69.2°, 74.2°, and 79.2°C, the limiting compliance, J_e , appears to have been reached and at 64.2°C a good estimate of it can be obtained. These values are listed

in Table I. It is clear that magnitude or vertical shifts along with time-scale shifts occur as the temperature is changed. Since we have no theory to guide us in predicting the form of the temperature dependence of the amplitude changes, we ideally should have some direct measure of the short-time limiting levels of this transition along with the J_e values before a temperature reduction procedure can be applied to this data. The short-time limiting levels of this mechanism will, of course, be a measure of the long-time limiting values of a preceding transition (assuming little or no overlap of contributions from different mechanisms) or of the temperature dependence of a true glassy compliance, J_g , which would reflect solely the bending or stretching of intra- and inter-molecular bonds. For TONB, it will be seen that a preceding viscoelastic mechanism is present. It was observed that the form of these curves, prior to a rather abrupt approach to the J_e level, was well described by the Andrade creep¹³⁻¹⁹ equation $J_r(t) = J_A + \beta t^{1/3}$; see Fig. 4 which is a linear plot of $J_r(t)$ as a function of $t^{1/3}$. Other measurements and further analysis, to be described later, are in accord with the presence of this kind of terminating Andrade creep. Meyer and Ferry have also observed this kind of response from glucose.⁵ It is therefore concluded that the extrapolated intercept, J_A , is the short-time limiting level of the preceding viscoelastic transition. With the values of these limiting compliances listed in Table I, the following amplitude reduction formula can be applied.*

$$J_R(t) = \frac{(J_e)_{T_0} - (J_A)_{T_0}}{J_e - J_A} [J_r(t) - J_A] + (J_A)_{T_0} \quad (1)$$

*This formula is analogous to the temperature and pressure reduction expression described by McKinney, Belcher, and Marvin for dynamic bulk compressibility measurements.²⁰

The constants without subscript pertain to the temperature of measurement and those with the subscript to the reference temperature, T_0 , to which all the data is reduced. Figure 5 indicates schematically the effect of temperature on a single viscoelastic dispersion. To achieve superposition at T_0 after the amplitude temperature dependence has been accounted for, all times must be divided by an empirical shift factor, a_T , at each temperature of measurement. Figure 6 shows the result of application of the described reduction to the chosen reference temperature, $T_0 = 64.2^\circ\text{C}$. The reduction is satisfactory and most of the entire transition is seen in just under five decades of reduced time. Instead of the amplitude range of 10,000 often observed in the response of polymers in their glasslike to rubberlike transition, a very modest change in compliance of 2.5 fold is seen here. On the other hand, the five-decade wide dispersion is (as will be seen below) indicative of an unexpectedly broad distribution function of retardation times, L , for such a small molecule as TCNB. Other glass-forming small molecules, which are about as bulky, have been reported to exhibit spectra which are claimed to be close to a single relaxation time.^{1,7} The measurements reported here indicate that such claims may be unjustified.

Creep and Recovery Measurements Along a Specified Glassy Volume Line

Often, when mechanical properties of glassy materials are measured, little if any attention is paid to identifying the non-equilibrium state that is being studied. We have attempted to establish by a fixed procedure, with accompanying dilatometric measurements, the volume-temperature line along which the creep and recovery measurements reported in this section were made. It is widely acknowledged that the same liquid configurational state is maintained along a single volume-temperature glass line. To reach volume equilibrium at some temperature below the conventional T_g , where contraction processes would be appreciably slowed down, the instrument was thermostated at 64°C for four days to insure volume equilibration. Subsequently, the instrument was cooled (ca. one deg./min.) to 39°C. This sizable temperature jump was made to reach a temperature where the rate of contraction was exceedingly minute and measurements could be taken over a period of a week at 39°C and lower temperatures while remaining sensibly on the same glassy volume line. Over the first 24-hour period at 39°C, the rate of creep diminished only one per cent testifying to negligible contraction during this initial period when the free volume collapse is most rapid. Succeeding measurements were made at increasingly lower temperatures. During the initial stages of this investigation at temperatures below T_g , it was felt that the sample density could be deduced from separate dilatometric measurements. It was discovered that the uncertainties involved in such deductions were too great for clear-cut interpretation. The obvious

and most effective method of following density of the sample by keeping a dilatometer in the instrument bath was eventually adopted. Our most extensive sojourn below T_g was monitored in this manner. Unfortunately, the series of creep measurements carried out during isothermal contraction were not. Consequently, densities had to be estimated from a separate series of dilatometric measurements.

Specific volumes determined along two glass lines are presented in Fig. 7. The upper line [$v_g(T^\circ\text{C}) = 0.867_2 + 1.4_0 \times 10^{-4}(T - 69)$, $T < 69$] is the conventional curve measured during one degree per minute cooling. Creep measurements were made along the lower line [$v_g(T^\circ\text{C}) = 0.863_3 + 1.4_8 \times 10^{-4}(T - 60)$, $T < 60$]. It is surprising that the T_g for the latter line turned out to be 60°C (see Fig. 7), in spite of the equilibration at 64°C . To obtain a measurement at 49.2°C , where the rate of contraction was greater, the instrument temperature was raised from 39.3°C ; creep was then measured for about a half hour; and the temperature was immediately lowered. A creep compliance check run at 39.3°C agreed to within one percent and the volume to within a few hundredths of a per cent. The results obtained at 49.2°C are therefore taken to represent behavior along the same glass line.

The creep compliance curves obtained at volumes along the lower glass line in Fig. 7 are shown in Fig. 8, together with the 64.2°C reference temperature curve. The two series of measurements taken along the lower glassy volume line were chronologically:

- 1) 64.2° , 39.3° , 34.3° , 29.4° , and 24.2°C ; 2) 64.2° , 39.3° , 49.2° , 39.3° , and 14.2°C . Both series of runs terminated when the weak brittle speci-

men cracked. The vertical position of the 14.2° curve was empirically determined using an extrapolated value of the temperature shift factor. This procedure was necessary because the calculated results fell about 10% too high and no subsequent check run was available to aid us in fixing its level. Although this apparent increase was probably caused by a partial failure of the sample interface bond, the shape of the response appears to be unaffected.

The creep behavior observed at 49.2°C and lower temperatures is indeed slight in this glassy region. All of these compliance curves shown in Fig. 8 indicate that little flow has taken place during the creep runs which are up to one day in length. During the 1200 seconds of creep at 49.2° viscous flow accounted for less than 4% of the total deformation. At 29.4° a viscous contribution was not detectable. Therefore the prolonged time dependence observed is viscoelastic and recoverable in nature. The recoverable compliances adjusted to a common Andrade intercept $[J(t) + \Delta J_A - \frac{t}{\eta}]$, where $\Delta J_A = J_A(64.2^\circ\text{C}) - J_A(T)$ are plotted as a function of the cube root of time, $t^{1/3}$, in Fig. 9. Here we see the short time limit to the domination of Andrade creep. The initial curvature indicates the presence of a preceding viscoelastic dispersion. In spite of the low level of compliances measured, at no temperature is there a definite approach to a time independent glassy compliance, J_g . The lack of a clear cut indication of what J_g may be can also be seen in Fig. 8.

For these measurements, made at non-equilibrium volumes, no information is available concerning the J_e levels. Extrapolation of

J_e values determined at higher temperatures is not possible because values so obtained would apply to the material at equilibrium densities. J_e must change in a manner similar to that of J_A . The less severe temperature dependence of J_A for the non-equilibrium glass is seen in Fig. 10. The change is from 0.1 to 2% per degree. That the amplitude of a compliance should change less with temperature when accompanied by a smaller rate of volume decrease is entirely reasonable since the level arises from the magnitude of intermolecular interactions. To reduce the data shown in Fig. 8, we can do little more with regard to the amplitude reduction than we have done in Fig. 9. The correct procedure described above must be in part abandoned. To an extent proportional to the change of J_e with temperature along the glassy volume line, the time shift factors, a_T , are in error, but because, as was just deduced, J_e changes very little with temperature we have reason to hope that the error is small. It must not be forgotten that slight amplitude errors can result in large-time shift errors when the time dependence is small, as it is in the region of glassy behavior. It is important to note that the curvature in a logarithmic plot is small for such behavior, and therefore the effect of the amplitude errors on the shape of the resulting master curve is usually negligible. The time-scale shift factors were calculated from the Andrade coefficient β ($a_T^{1/3} = \beta_0/\beta$, where β_0 is the value at the reference temperature).¹⁸ No attempt has been made to estimate corrections for the amplitude temperature dependence.

The data from four of the curves presented in Fig. 9 were plotted logarithmically on a reduced time scale. The values of J_A and

a_T found are given in Table 2. The resulting "master" curve of the reduced recoverable compliance, $J_R(t)$, at 64.2°C is displayed in Fig. 11, together with smoothed values read from the reduced curve determined at equilibrium volumes; see Fig. 6. The superposition procedure appears to be successful over the entire range of measurement. Within experimental error, all of the viscoelastic mechanisms involved have the same temperature dependence.²¹

The Retardation Spectrum

Presented also in Fig. 11 are the results of second approximation calculations of the retardation spectrum, L_2 , cm²/dyne. Two different approximation equations were used on the curve from Fig. 6 (the reduced response observed at equilibrium volume). The open circles were obtained using Leaderman's²² expression and the circles with the external pips with the Stern²³ adaptation of the Ferry-Williams²⁴ method. Separate calculations were made on each of the four lower temperature curves in an attempt to avoid the influence of a single averaging line drawn through all the $J_R(t)$ points. The low slopes observed in this region makes such calculations extremely sensitive to small variations in the accepted line. Only Leaderman's method was used on these curves.

As the recoverable compliance, $J_R(t)$, approaches the steady state compliance, J_e , the retardation spectrum drops to zero. To the left of the observed peak, which is some three orders of magnitude lower than peaks observed in polymeric systems, L_2 has a slope of 1/3 for about three decades of time. This is a reflection of the

linearity of $J_r(t)$ with $t^{1/3}$ mentioned above. At still shorter times, L_2 definitely tends to level out to a plateau, and finally between 10^{-5} and 10^{-4} it appears to drop off again. The drop-off at short times should be regarded with suspicion since it reflects the region of least accuracy and is dependent on but a few of the 14.2° points.

The spectrum clearly indicates the presence of two groups of viscoelastic mechanisms. At reduced times, larger than 0.1 second a terminating form of Andrade creep dominates the recoverable response. Although Andrade creep has been observed in a wide variety of materials, from metals¹³⁻¹⁶ to amorphous glassy²⁵ and rubbery^{18,19} polymers, very little progress has been made toward an understanding of the underlying process.^{16,26} The fact that the temperature dependences of J_A and J_e differ tend to confirm that the plateau at the shorter times represents a second kind of response. It is therefore suggested, that the total creep compliance is represented by

$$J(t) = J_g + J_A \psi_A(t) + J_e \psi_e(t) + \frac{t}{\eta}$$

where the glassy compliance, J_g , appears to be about $8 \times 10^{-11} \text{ cm}^2/\text{dyne}$ for TONB and $\psi_A(t)$ and $\psi_e(t)$ are normalized retardation functions. The linear term in time, t , as usual describes the viscous contribution to the deformation.

Specific Volume Temperature Dependence

Specific volume measurements between 25° and 310°C on TONB have been reported by Magill and Ubbelohde.⁹ Their dilatometric measurements were carried out by equilibrating for 1/2 hour at temperatures spaced on the average about ten degrees apart except for the neighborhood of most rapid crystallization. To confirm the position of the glass transition temperature, T_g , in this study, relative measurements of volume were made dilatometrically between 29° and 116°C. During these determinations the thermostat was cooled at a rate of 1 to 2°C per minute. Several cycles were carried out and the absolute values of specific volume were fixed by matching against the earlier results well above T_g . Following a suggestion of Professor John Lamb,²⁷ that over wide ranges of temperature the density, ρ , of a liquid is a more linear function than the specific volume, we have plotted both sets of data in Fig. 12 as the density. Within experimental error, the results are indeed linear from the glass temperature, $T_g = 69^\circ\text{C}$, up to the highest temperature of measurement, 244°C. Only two points are more than 0.1% from the line

$$\rho(T^\circ\text{C}) = 1.1348 - 6.06 \times 10^{-4} (T-100) \quad T > 69 \quad (2)$$

ρ is in g/cm^3 . The results over the much smaller temperature range below T_g can be described equally well in terms of volumes. The older results⁹ are represented by the larger circles. Open and half-filled circles distinguish between the results obtained in the two different dilatometers that were necessary to cover the large temperature range. Results obtained in the present study are represented by the small circles. Log v values

are also shown plotted against the temperature in Fig. 12. The curvature in this line indicates that the thermal expansion coefficient is not constant, but increases appreciably between T_g and $T_g + 100^\circ\text{C}$.

Specific Volume Time Dependence

In addition to determining the glass line, established by thermostating at 64° for four days, isothermal volume contraction measurements were made after the manner of Kovacs.²⁸ The dilatometer was equilibrated at 80° for each measurement; after which it was quickly transferred to a neighboring bath that was regulating at the temperature of measurement. The time dependent results for two temperatures, 49.2 and 59.2°C are shown in Fig. 13 plotted as the fractional deviation from the equilibrium volume, $V - V_\infty / V_\infty$, versus the logarithm of time; V_∞ is the equilibrium volume. Two sets of measurements were carried out at each temperature to assess the reproducibility.

Creep During Isothermal Volume Concentration

At temperatures appreciably below 59°C the time to reach the super-cooled liquids time-independent density becomes impractically long. At the same time, the rate of volume concentration is slow enough to permit rather extensive measurement of the effect of this contraction on the isothermal creep behavior. Therefore, after reaching metastable equilibrium at 59.2°C as described above (Fig. 1) temperature of the sample was lowered to 49.2°C and a series of measurements was started. The results of the series are depicted in Fig. 14. Runs A, B, C, D, and E were taken on the first, second, third, fifth, and eighth days at 49.2°C , respectively. The sevenfold decrease in rate of creep

observed here is clearly a function only of the decrease in free volume and will be correlated with estimates of the concurrent volume contraction. Since the intermolecular forces involved are functions of distance, a small decrease in the amplitude of response is expected with the slight decrease in volume that occurred, but our precision during this series of runs was not great enough to resolve it. Within the experimental scatter, a simple time scale shift is all that was observed. There was no appreciable effect on the shape of the compliance curves by contraction during the runs beyond the first day. The measured shifts are recorded in Table 3.

Temperature Dependence of the Viscosity

Above 80°C only the non-recoverable contribution to the deformation could be measured with accuracy. At higher temperatures the torsional creep apparatus was therefore utilized as a rotational viscometer. The liquid cylinder geometry was employed for all these measurements. At the highest temperatures of measurement the 3.2 cm diameter sample plates were used. Our present measurements extended to 200°C overlapping the earlier capillary measurements of Magill and Ubbelohde by some 15°. Values of the viscosity at temperatures below 80° were determined, where possible, from steady state angular velocities of the moving plate. At temperatures where steady state deformation was not reached, viscosities were calculated from differences between creep and recovery. Our results obtained at metastable equilibrium densities are plotted (open circles) in Figure 15 along with those from reference 9 (filled circles) as a function of temperature. The position of the conventional glass temperature, T_g , is indicated. It is significant to note that so long as conditions of metastable equilibrium

are maintained, the second derivative of the curve remains positive, i.e., no point of inflection is observed in the neighborhood of T_g as is often reported in the literature. In addition, the value of $\log \eta$ at T_g is about 11.3, not 13. The latter is the often quoted rule of thumb value. The value of 13 even overestimates the viscosity of a non-polar polymer like polystyrene²⁹ (molecular weight $\approx 47,000$). $\log \eta$ values are shown in Table 4 with the temperatures of measurement.

Free Volume Analysis

Starting with the Doolittle expression³⁰ for the dependence of the viscosity on the relative free volume,

$$\ln \eta = \ln A + \frac{Bv_o}{v_f} \quad (3)$$

where A and B are characteristic material constants and v_o and v_f are the occupied volume and the free volume, $v - v_o$, respectively

Williams, Landel, and Ferry derived³¹ an equation of the form

$$\log a_T = -c_1(T - T_g)/(c_2 + T - T_g) \quad (4)$$

which was empirically found to fit the temperature dependence of viscous, viscoelastic, and dielectric behavior of a wide variety of glass-forming materials. They also pointed out that this form was implied by Vogel's equation³²

$$\ln \eta = \ln a + c/(T - T_\infty) \quad (5)$$

In their derivation they assumed that the temperature dependence of the fractional free volume, $f = (v - v_o)/v$, was equal to $f_g + \alpha_f(T - T_g)$, where f_g is the value of f at the glass temperature and $\alpha_f = \alpha_\ell - \alpha_g$, is the difference between the cubic thermal expansion coefficients for the super-cooled liquid, α_ℓ , and the glass, α_g . The glassy expansion coefficient is taken to be a measure of that of the occupied volume α_o . The Doolittle constant, B was also assumed equal to unity. The additional assumption

that $v_f/v \approx v_f/v_o$ was unnecessary since $\frac{v_{o,1}}{v_{f,1}} - \frac{v_{o,2}}{v_{f,2}} = \frac{v_1}{v_{f,1}} - \frac{v_2}{v_{f,2}}$,

where the subscripts 1 and 2 indicate values of v_o and v_f at two temperatures.³³ The resulting constants c_1 and c_2 are $1/2.303f_g$ and f_g/α_f as given by WLF, and $c/2.303\Delta$ and Δ in terms of Vogel equation constants³⁴ where $\Delta = T_g - T_\infty$.

Anticipating the results obtained below, we show our experimental evidence supporting the assumption Williams made at a later date³⁵ to allow B to assume values other than one. This is that $\alpha_f = \alpha_l$; i.e., $\alpha_o = 0$. In terms of $\log a_T$ the temperature dependences of the viscosity of the supercooled liquid, filled circles, (here $\log a_T = \log \eta(T) - \log \eta(64.2)$) and the retarded recoverable compliance of the specified glass, open circles, are shown in Fig. 16 as a function of temperature. In Tables 1 and 2 the $\log a_T$ values obtained for both processes at several temperatures only differ by 0.2 or less. With our present data we can only conclude that these differences are within experimental error and these two contributions to the creep compliance have the same temperature dependence. The solid line for the metastable liquid and the dashed line for the unstable glass have been calculated assuming that the thermal expansion coefficient of the occupied volume, α_o , is zero. The dotted horizontal line represents the application of the WLF model, admittedly into the region below T_g , where it was claimed not to apply. We will attempt to show that such an apparent

limitation of the free volume approach is not necessary. Rather than obtain a better fit to the data with the unpalatable assumption of a negative α_o we conclude the imperfect fit is due to experimental uncertainty. In any event, it is clear that $\alpha_o \ll \alpha_g$.

Since v_o can be concluded to be insensitive to temperature, then assuming volume-temperature linearity

$$v = v_{T_g} + \frac{dv}{dT} (T - T_g) \quad (6)$$

with equation (3) the following expression can be derived

$$\log a_T = -(B/2.303 \phi_g)(T - T_g) / \left[(\phi_g v_o \frac{dv}{dT}) + T - T_g \right] \quad (7)$$

The relative free volume, $\frac{v - v_o}{v_o}$, is

$$\phi = \phi_g + \frac{1}{v_o} \frac{dv}{dT} (T - T_g) \quad (8)$$

where ϕ_g is its value at T_g .

Vogel equation constants were first obtained with the viscosity data to determine the range of free volume domination. The resulting expression was obtained:

$$\log \eta = -17.46 + 4.10 \times 10^3 (T - 200)^{-1} \quad (9)$$

Temperature is expressed in °K. This equation describes the viscosity behavior below 120°C and the dashed line in Figure 15 illustrates the departure from observed values at higher temperatures. At the conventional T_g of 69°C the WLF parameters f_g and α_f are 0.015 and 1.06×10^{-4} , respectively, which we present for comparison with the "universal" values of 0.025 and 4.8×10^{-4} . The measured difference $\alpha_\ell - \alpha_g$ is 4.4×10^{-4} for TONB; $\alpha_\ell (69^\circ) = 5.0 \times 10^{-4}$.

Fig. 17 schematically represents the free volume picture required by a temperature independent v_o . If we ignore the non-linearity of the volume-temperature dependence of TONB, the slope, $\frac{dv}{dT} = 4.54 \times 10^{-4}$, at T_g can be used to extrapolate the metastable liquid line to $T_\infty = 200^\circ\text{K}$ where the free volume is zero. Such an extrapolation yields a $v_o = 0.802 \text{ cm}^3/\text{g}$ which implies a $\phi_g = 0.081$ and $B = 5.5$ from $B = c\phi_g/\Delta$. However, since the density is a linear function of temperature for TONB above T_g , equation (2) yields a more realistic value of v_o at T_∞ . The result for v_o is 0.807 and ϕ_g and B become 0.074 and 4.9, respectively. Even this procedure, which uses the T_∞ obtained by fitting the Vogel equation to the data, is an approximation to the extent that the volume is non-linear in the temperature range where the pertinent viscosity values were obtained.

With specific volume data available, the Doolittle equation (3) can be used directly to analyze the shift factor data, thereby avoiding assumption (both explicit and implicit) of volume-temperature linearity. A reference volume, v_g , is chosen, where $J(t)$ or η has been measured and the straight line expression

$$\frac{v_s - v}{\log a_T} = \frac{2.303(v_s - v_o)}{Bv_o} (v - v_o) \quad (10)$$

is used. A plot of $(v_s - v)/\log a_T$ versus v yields the constants v_o and B from the slope and intercept. This procedure is analogous to the Ferry temperature plot²¹ of $T - T_s/\log a_T$ against $T - T_s$ which yields the WLF constants c_1 and c_2 . A severe test of free volume concepts can be applied by comparing the results obtained in the different accessible regions of the phase diagram (Figure 17) with equation (10). The data are shown in Figure 18 plotted twice, with a different chosen reference volume in each instance, to illustrate the amplification of errors near v_s . The filled circles on the $v_s - v/\log a_T$ versus v plot represent the viscosity results obtained on the metastable liquid. The half black circles were obtained from the specified glass and the open circles during isothermal volume contraction at 49.2°C. The values of v_o and B deduced from the $v_s = 0.8651 \text{ cm}^3/\text{g}$ line are $0.810 \text{ cm}^3/\text{g}$ and 4.23; from the $v_s = 0.8831 \text{ cm}^3/\text{g}$ line, $0.811 \text{ cm}^3/\text{g}$ and 4.13, respectively. The resulting ϕ_g at 69°C is 0.070. These last values are taken to be the best characterizing constants especially since it appears clear that, within our experimental error, all of our results are adequately represented with the exception of the viscosities measured above 120°C, where the relative free volume is not the sole determining factor. To this extent, the free volume concept is substantiated. The other values given above should be indicative of the magnitude of errors introduced by the several assumptions mentioned. The accepted temperature dependence equation, relative to the established T_g of 60°C, is

25.

$$\log a_T = 1.81 \left[\frac{v}{v-0.810_5} - \frac{0.8633}{0.0528} \right] . \quad (11)$$

DISCUSSION

Previous attempts to rationalize the severe temperature dependence of relaxation processes in the neighborhood of the glass transition temperature in terms of free volume concepts have generally rested on assumptions concerning α_0 and arbitrary definitions of v_0 . These contributions have been thoroughly examined in an extensive review by Kovacs.²⁸ It has been assumed here that the Doolittle expression³⁰ is correct in form and that a temperature insensitive v_0 is operationally determined by the temperature response of a property which is dominated by a single kind of molecular mechanism. The occupied volume, v_0 , is therefore to be considered a measure of the volume which is unavailable for the pertinent molecular process. For example, the volume requirements for rotation of a molecule must depend on its shape and the possible directional nature of its interactions with its neighbors. The requirements for translation, a priori, are not necessarily the same, unless translation can only occur by means of cooperative rotation. This appears to be an unlikely circumstance in general. Utilizing the analysis presented in this paper, one of us has found²⁹ that the retarded elastic compliance and the viscosity of polystyrene have different effective occupied volumes.

It appears reasonable to us that the concept of molecular motion, being hindered by crowded conditions, can be treated in terms of density fluctuations³⁶ or equivalently in statistical mechanical terms of a small number of available configurations of the system in phase space. The latter approach is exemplified by the recently proposed theory of Adam and Gibbs.³⁷ Though appealing and apparently successful, it suffers from the

defect that it predicts no time scale shift so long as a particular average liquid configuration is maintained. It has been widely acknowledged by many, including Adam and Gibbs,³⁷⁻⁴⁰ that the liquid configuration does not change along a glass volume-temperature line. Our creep measurements made along such a line have a temperature dependence that is by no means small. The free volume, therefore, appears to be the pertinent variable. At least to a first approximation, whether a decrease in ϕ is the result of more efficient molecular packing, or simply the consequence of a decrease in the amplitude of thermal vibrations does not seem to matter. A statistical mechanical explanation will have to include the effect of vibration amplitude on the number of possible configurational states.

CONCLUSIONS

Creep recovery measurements of TONB have revealed an unexpectedly broad retardation spectrum (greater than 9 logarithmic decades) which indicates the presence of two contributing groups of retardation mechanisms; one of which gives rise to a terminating Andrade creep response. The amplitude of the retarded recoverable compliance increases with increasing temperature at a much greater rate above T_g . Recoverable creep compliance results, measured both above and below T_g , have been reduced to a single composite curve at 64.2°C over an enhanced time scale. Within experimental uncertainty the temperature dependence of η and $J_r(t)$ are the same. So long as η was determined while TONB was at a metastable equilibrium density no point of inflection in the plot $\log \eta$ versus temperature was observed. The density of TONB was found to be a linear function of temperature between T_g and 244°C. The value of the viscosity and the position of the retardation spectrum on the time scale were found to be functions of the volume per se. In applying free volume theory to the results it was deduced that $\alpha_0 \simeq 0$.

ACKNOWLEDGEMENTS

D. J. Plazek thanks NASA under Grant NsG 147-61, and J. H. Magill acknowledges support from ONR under Contract No. Nonr 2693(00) during these investigations. The authors gratefully acknowledge Franklin L. Miller's assistance with the calculations.

TABLE 1

Characterizing Parameters at Equilibrium Volume

T°C	J_A $\times 10^{10}$ cm ² /dyne	J_e $\times 10^{10}$ cm ² /dyne	log a_T^a	log a_T^b	log β
64.2	0.85	2.58	0	0	-10.77 ₂
66.5	0.90	2.76	---	-0.50 ₀	---
69.2	0.950	2.83	-0.98 ₃	-1.03 ₇	-10.40 ₄
74.2	1.15	3.21	-1.84 ₀	-1.94 ₆	-10.15
79.2	1.5	3.53	-2.66 ₃	-2.86 ₇	- 9.82

a. from retarded compliance

b. from viscosity

TABLE 2

Characterizing Parameters Along Specified Glass Line

$T^{\circ}\text{C}$	$J_A \times 10^{10}$ cm^2/dyne	$\log \eta$	$\log a_T^a$	$\log \beta$	$\log a_T^b$
24.2	0.81	---	---	-12.30_1	4.60
29.4	0.82	---	---	-12.16_4	4.18
34.3	0.83	16.20	3.85	-11.98_5	3.65
39.2	0.83	15.47	3.12	-11.74_6	2.93
49.2	0.84	14.52	2.17	-11.536	2.30

a. from viscosity

b. from β

TABLE 3

Characterizing Parameters During Isothermal Contraction

Time ^a sec. $\times 10^{-3}$	T°C	v cm ³ /g	$\frac{J_A}{x} 10^{10}$ cm ² /dyne	log a _T ^b	log β	log a _T ^c
4	49.2	0.8619	0.84	2.19	-11.53	2.28
87	49.2	0.8603	0.84	2.49	-11.63	2.58
184	49.2	0.8598		2.72		
353	49.2	0.8594		2.88		
634	49.2	0.8593	0.84	3.03	-11.81	3.12
4	59.2	0.8640	0.92	0.83	-11.02 ₈	0.78
76	59.2	0.8630	0.91	1.08	-11.10 ₅	1.01
310	59.2	0.8629	0.92	1.12	-11.10 ₅	1.01

a. Time of start of run after temperature equilibrium.

b. From viscosity.

c. From β .

TABLE 4

Viscosity Temperature Dependence^a

T°C	log η ^b	T°C	log η	T°C	log η
59.2	13.47	104.2	5.58	192.6	-0.274
64.2	12.35	109.2	4.93	199.8	-0.398
66.5	11.85	114.2	4.33	210.0	-0.569
69.2	11.29 ₅	124.3	3.27	222.4	-0.779
74.0	10.39	144.3	1.65	238.5	-0.984
79.2	9.46 ₅	160.0	0.81	277.0	-1.360
84.2	8.56 ₅	169.7	0.37 ₅	287.7	-1.419
89.2	7.76 ₅	184.8	-0.076	298.5	-1.497
94.2	7.05 ₅	189.0	-0.170	310.6	-1.561
99.2	6.25	191.8	-0.258		

a. Values at 184.8°C and above are the capillary values of Magill and Ubbelohde. Tabulated values were not given in reference 9.

b. Viscosity values are in Poise (dyne sec./cm²).

REFERENCES

1. J. J. Benbow, Proc. Phys. Soc. B, 67, 120 (1954).
2. S. Crawford, Proc. Phys. Soc. B, 69, 1312 (1956).
3. A. L. Clark and T. A. Litovitz, J. Acoust. Soc. Amer., 32, 1221 (1960).
4. D. O. Miles, Phys. Fluids, 4, 1482 (1961).
5. H. H. Meyer and J. D. Ferry, Trans. Soc. Rheology, 9:2, 343 (1965).
6. V. Philippoff in W. Mason, ed., "Physical Acoustics", Vol. IIB, Academic Press, New York and London, 1965.
7. A. V. Tobolsky and R. B. Taylor, J. Phys. Chem., 67, 2439 (1963).
8. S. S. Pollack, unpublished measurements.
9. J. H. Magill and A. R. Ubbelohde, Trans. Faraday Soc., 54, 1811 (1958).
10. D. B. Clapp and A. A. Morton, J. Amer. Chem. Soc., 58, 2172 (1936).
11. H. O. Wirth, W. Kern, and E. Schmitz, Makromol. Chem. 68, 69 (1963).
12. V. J. MacCosham, "Conference on the Ultracentrifuge", Academic Press, Inc., New York, N. Y., 1963, p. 249.
13. E. N. da C. Andrade, Proc. Roy. Soc., London, A84, 1 (1910).
14. E. N. da C. Andrade, Phil. Mag., 7, 2003 (1962).
15. C. Henderson, Proc. Roy. Soc., A206, 72 (1951).
16. A. J. Kennedy, J. Mech. and Phys. Solids, 1, 172 (1953).
17. K. Van Holde, J. Polymer Sci., 24, 417 (1957).
18. D. J. Plazek, J. Colloid Sci., 15, 50 (1960).
19. D. J. Plazek, ibid., 16, 107 (1961).
20. J. E. McKinney, H. V. Belcher, and R. S. Marvin, Trans. Soc. Rheology, 4, 347 (1960).
21. J. D. Ferry, "Viscoelastic Properties of Polymers", John Wiley and Sons, Inc., New York, N. Y., 1961, Chapter 11.
22. H. Leaderman, in F. R. Birich, ed., "Rheology, Theory and Applications", Vol. 2, p. 49, Academic Press, New York, N. Y., 1958.

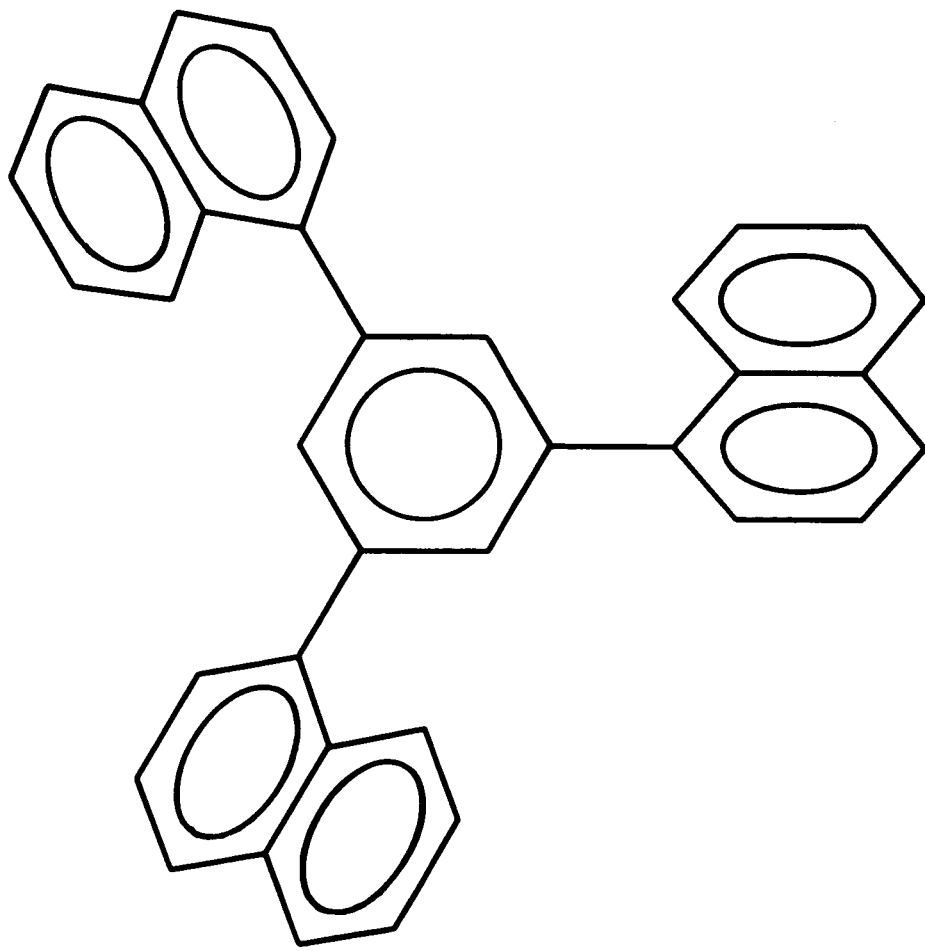
23. D. M. Stern, Ph.D. Thesis, University of Wisconsin, Madison, 1957.
24. M. L. Williams and J. D. Ferry, J. Polymer Sci., 11, 169 (1953).
25. D. R. Reid, Brit. Plastics, p. 2, October (1959).
26. N. F. Mott, Phil. Mag., 44, 742 (1953).
27. J. Lamb, private communication.
28. A. J. Kovacs, Fortschr. Hochpolym. Forschung., 3, 394 (1963).
29. D. J. Plazek, J. Phys. Chem., 69, 3480 (1965).
30. A. K. Doolittle, J. Applied Phys., 22, 1471 (1951); 23, 236 (1952).
31. M. L. Williams, R. F. Landel, and J. D. Ferry, J. Amer. Chem. Soc., 77, 13701 (1955).
32. H. Vogel, Physik Z., 22 645 (1921).
33. H. Markovitz, private communication.
34. T. G Fox and G. C. Berry, Fortschr. Hochpolym. Forschung., to be submitted.
35. M. L. Williams, J. Appl. Phys., 29, 1395 (1958).
36. M. H. Cohen and D. Turnbull, J. Chem. Phys., 31, 1164 (1959).
37. G. Adam and J. H. Gibbs, J. Chem. Phys. 43, 139 (1965).
38. W. Kauzmann, Chem. Rev., 43, 219 (1948).
39. G. O. Jones, Phys. Soc. Rep. Prog. Phys., 12, 131 (1948-49).
40. T. G Fox, Jr. and P. J. Flory, J. App. Phys., 21, 581 (1950).

LEGENDS

- Figure 1. Logarithmic plot of the creep compliance, $J(t)$ cm^2/dyne , of TONB as a function of time, t , in seconds. Measurements were taken during isothermal volume contraction at 59.2°C . Time interval at temperature before start of runs: \odot , 4×10^3 ; \circ , 76×10^3 ; \bullet , 310×10^3 sec. Retarded recoverable compliances, $J_r(t)$, of same runs plotted against the cube root of the time, $t^{1/3}$.
- Figure 2. Logarithmic plot of creep compliance, $J(t)$, as a function of time. TONB was at metastable equilibrium volume at indicated temperatures during these measurements.
- Figure 3. Logarithm of the recoverable creep compliance $J_r(t)$ presented as a function of the logarithm of time (t in seconds) at the indicated temperatures.
- Figure 4. Recoverable compliances from Figure 3 shown here as a function of the cube root of time, $t^{1/3}$.
- Figure 5. Schematic representation of the recoverable creep compliance versus log time at two temperatures to help illustrate the temperature reduction procedure of the amplitude dependence. As drawn, the reference temperature T_0 is the lower of the two.
- Figure 6. Logarithmic plot of the amplitude reduced recoverable creep compliance, $J_R(t)$, as a function of reduced time, t/a_T . All of the data are reduced to 64.2°C .
- Figure 7. Specific volume-temperature plot showing an extrapolation of the metastable equilibrium liquid line with two measured glass lines. The upper (conventional) glass line represents the result of 1°C per minute cooling and the lower line represents the specified glass as described in the text.
- Figure 8. Logarithmic presentation of the creep compliance curves, $J(t)$, of the specified glass of TONB at the indicated temperatures. The response at the reference temperature ($T_0 = 64.2^\circ\text{C}$, equilibrium volume) to which the data on the glass will be reduced is also shown.
- Figure 9. Linear plot of the recoverable compliance ($J_r(t) = J(t) - \frac{t}{\eta}$), adjusted to a common Andrade intercept ($\Delta J_A = J_A(64.2^\circ) - J_A(T^\circ)$) against the cube root of time, $t^{1/3}$, calculated from data presented in Figure 8.

- Figure 10. Dependence of the Andrade intercept compliance, J_A , of the specified glass and the metastable liquid on temperature, $T^\circ\text{C}$.
- Figure 11. Logarithm of the temperature reduced recoverable compliance, $J_R(t)$ as a function of the logarithmic reduced time, $\log t/a_T$. Open circles are from Fig. 6. Others are designated at four temperatures from the specified glass response, $T_0 = 64.2^\circ$. Also the logarithm of the second approximation to the retardation spectrum, L_2 . Open circles calculated with Leaderman's expression; circles with external pips with the Stern adaptation of the Williams-Ferry method; others derived from individual $J_R(t)$ curves, as indicated, with the former expression.
- Figure 12. Density and logarithm of the specific volume, v , shown as a function of temperature. Open and half-filled circles from reference 9; two different dilatometers. Filled small circles from present study.
- Figure 13. Fractional excess volume above equilibrium value, V_∞ , plotted as a function of logarithmic time at 49.2 and 49.2°C . Filled and open circles represent separate measurements.
- Figure 14. Logarithmic creep compliance-time plot. Measurements made during spontaneous volume contraction at 49.2° . Starting time periods after attainment of thermal equilibrium are given in text.
- Figure 15. Logarithm of the viscosity, η , plotted as a function of temperature. Conventional glass transition temperature, T_g , is indicated. Dashed line is calculated from Equation 9.
- Figure 16. Logarithm of time scale shift factors, a_T , plotted as a function of temperature. Solid line for metastable liquid and long-dash line for specified glass calculated with Equation 7 and the thermal expansion coefficient of the occupied volume, α_0 , assumed zero. Short-dash line represents the curve for $\alpha_0 = \alpha_g$. Filled circles from η ; open circles from $J_R(t)$ curves of the specified glass.
- Figure 17. Schematic representation of phase diagram depicting free volume parameters which are suggested by the data reported for TONB. Heavy solid lines correspond to measured results in this work and in Reference 9. Dashed lines are deduced. T_m is the melting point, $T_{g,s}$ and $T_{g,c}$ are the glass transitions temperatures for the specified and conventional glasses; T_∞ is the temperature at which a liquid at equilibrium density would possess zero free volume; and v_0 is the temperature insensitive occupied volume.

Figure 18. Ratio of volume difference from the chosen reference volume to the logarithm of the time scale shift factor, $v_s - v / \log a_T$, plotted against the specific volume for two different values of v_s . Filled circles from measurements on metastable liquid; top dark circles from specific glass response; and open circles from measurements during isothermal volume contraction at 49.2°C.



1,3,5 Tri- α -Naphthyl Benzene

$T_m = 199^\circ\text{C}$

$T_g = 69^\circ\text{C}$

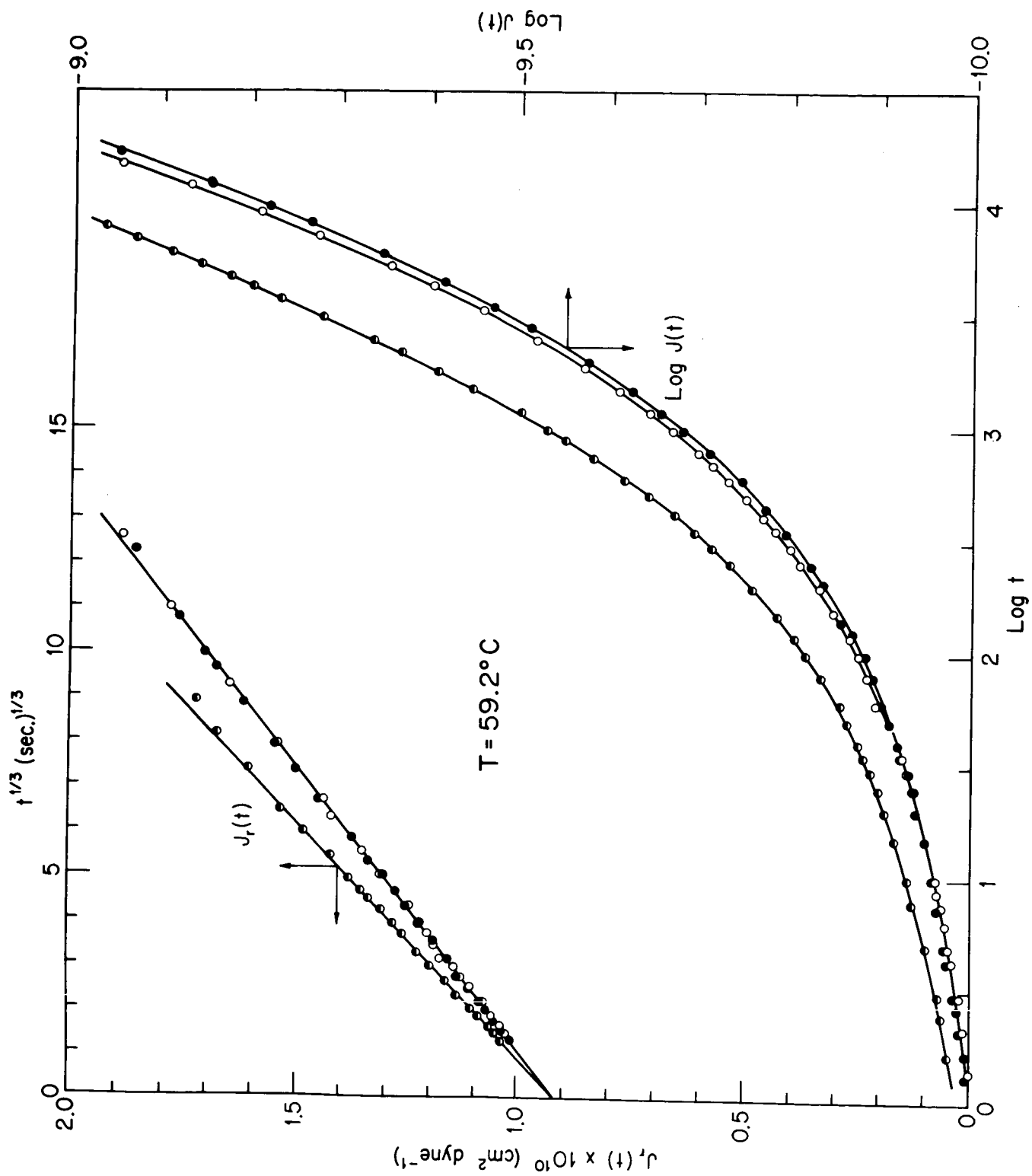


Figure 1

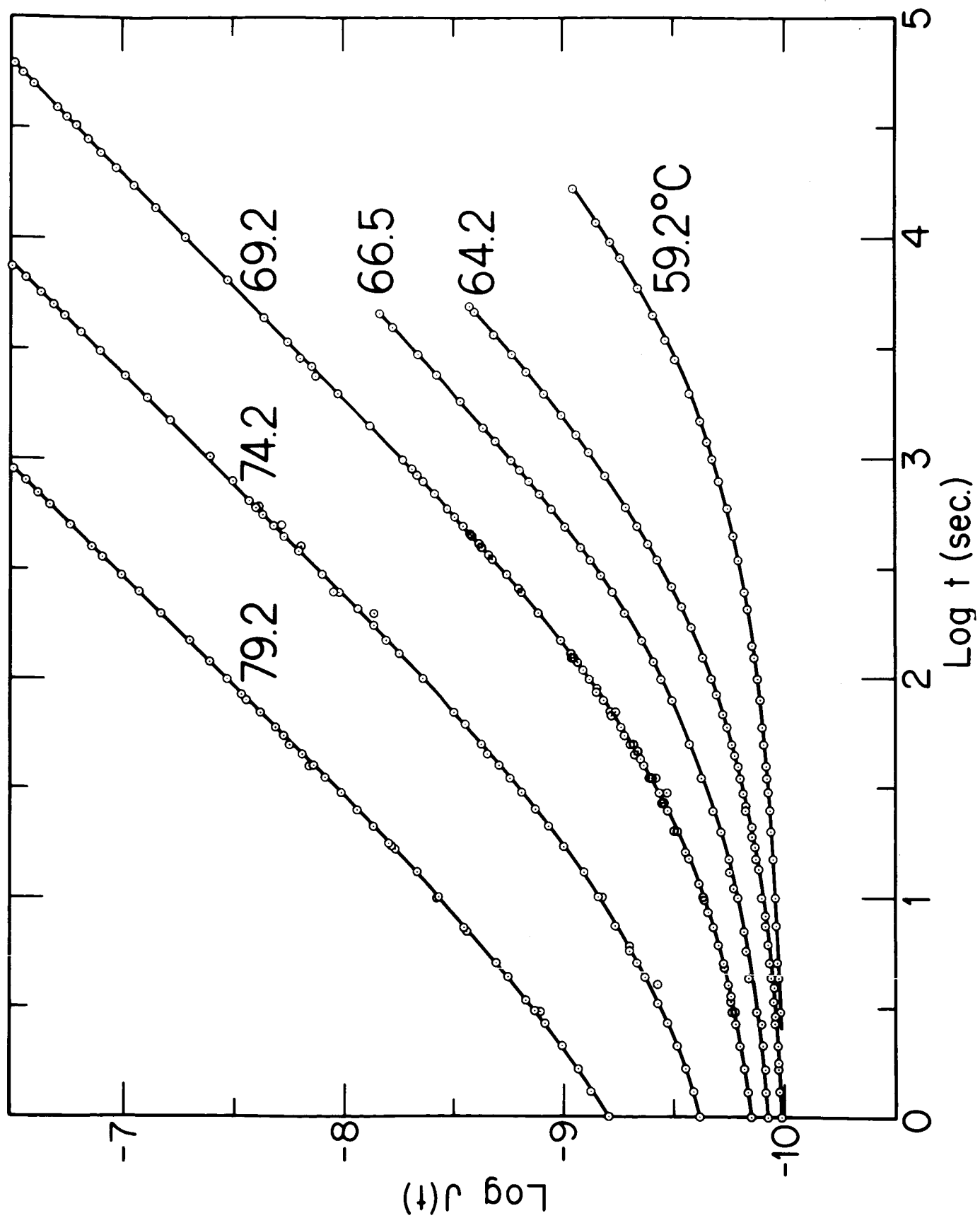


Figure 2

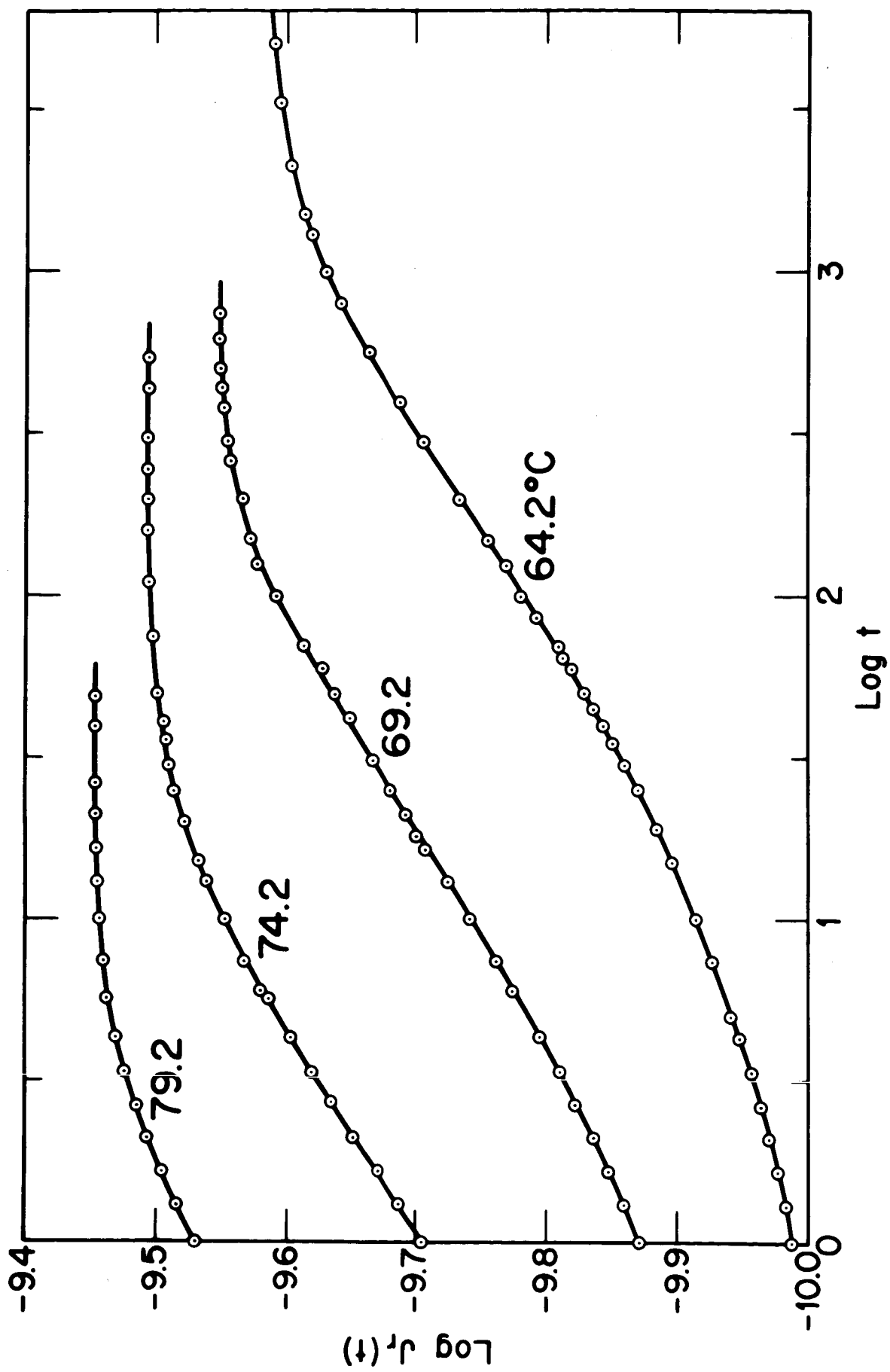


Figure 3

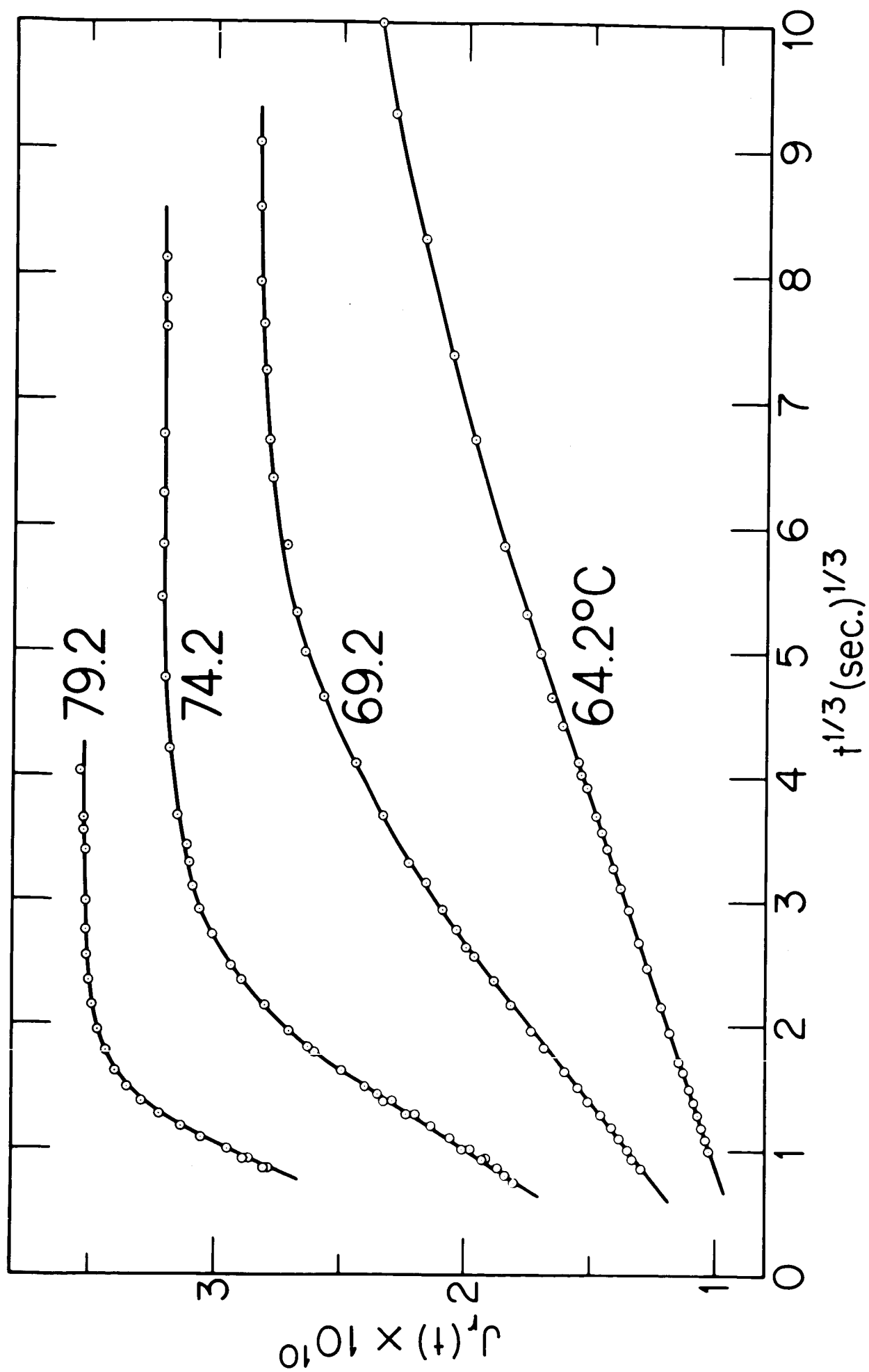


Figure 4

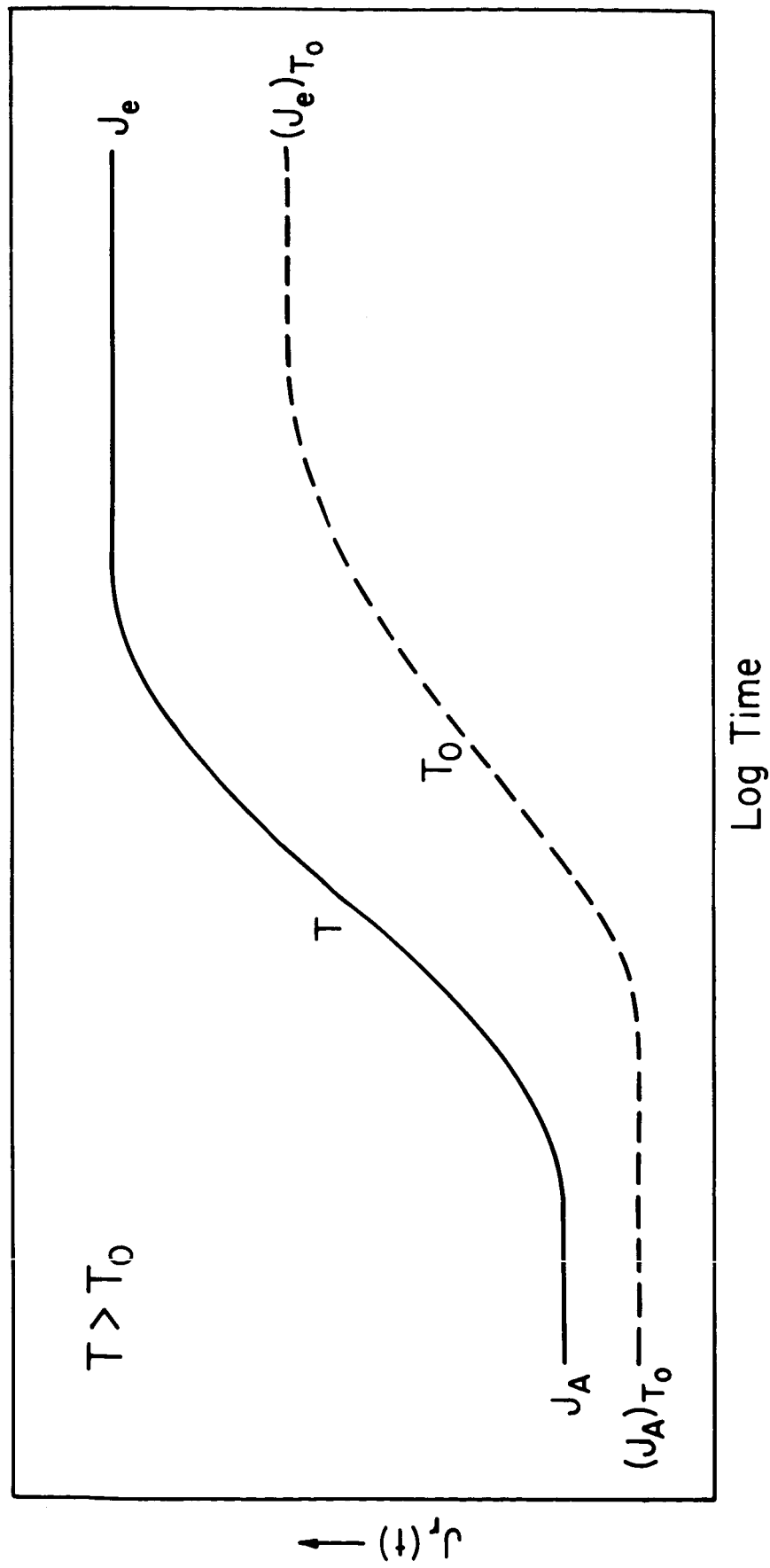


Figure 5

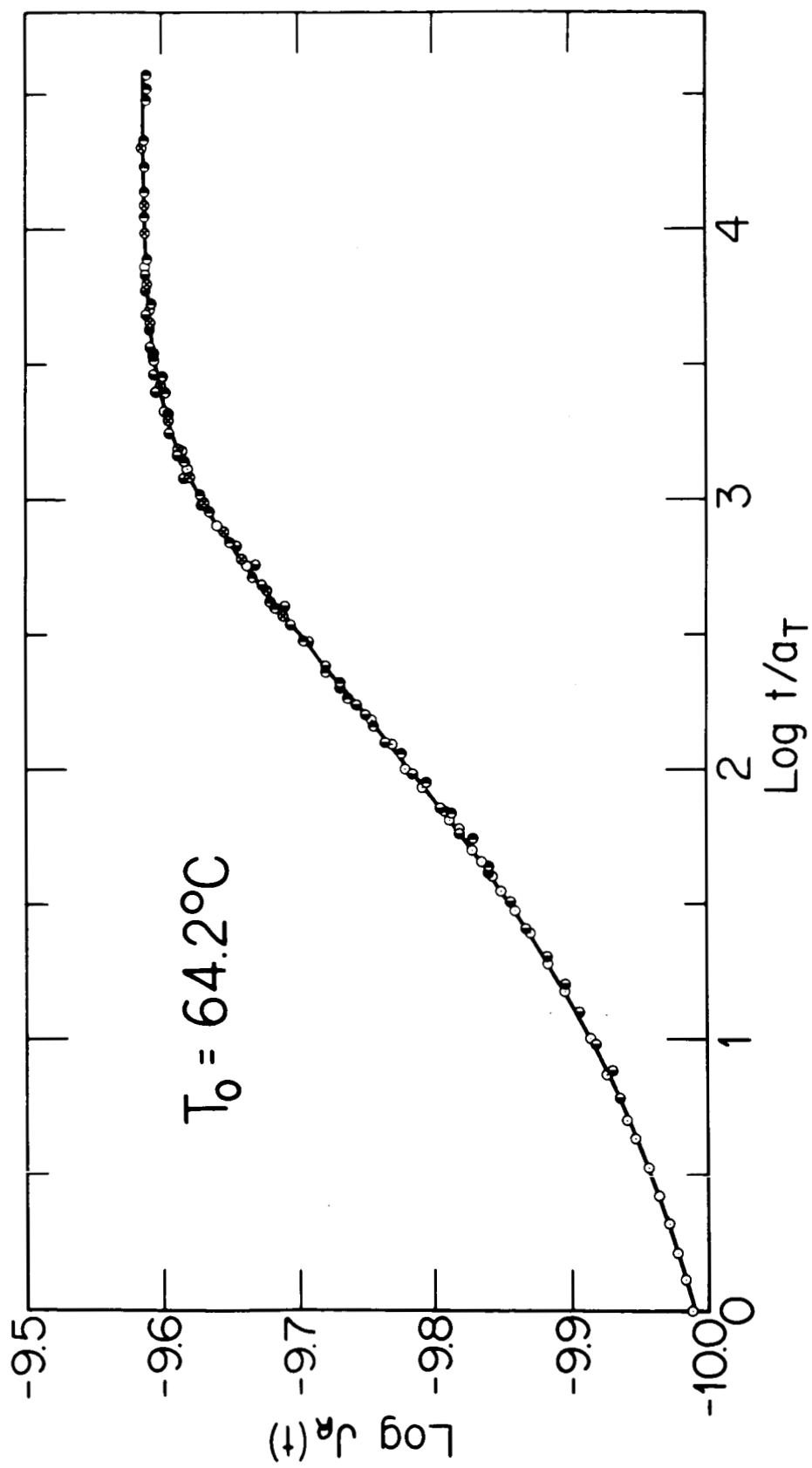


Figure 6

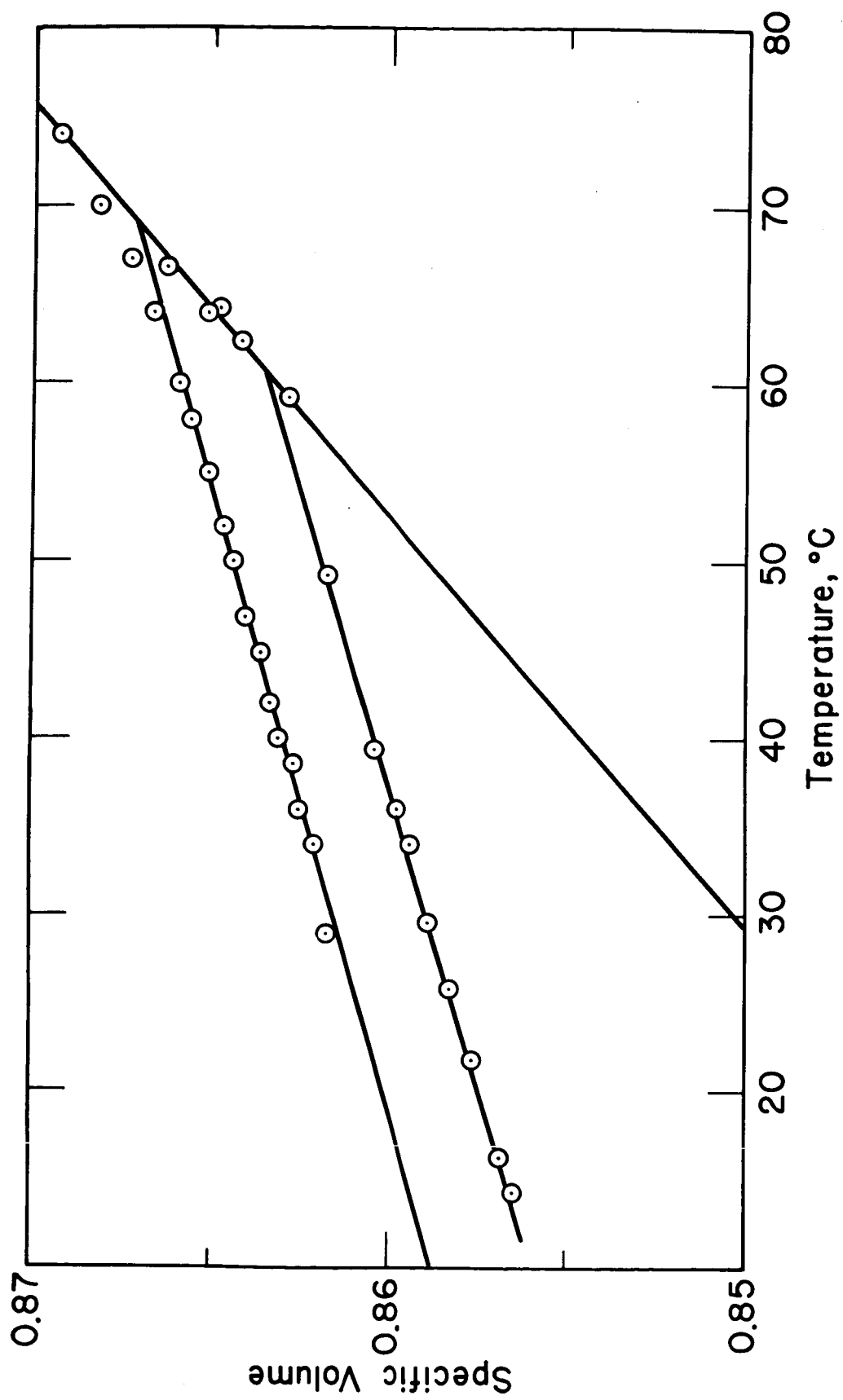


Figure 7

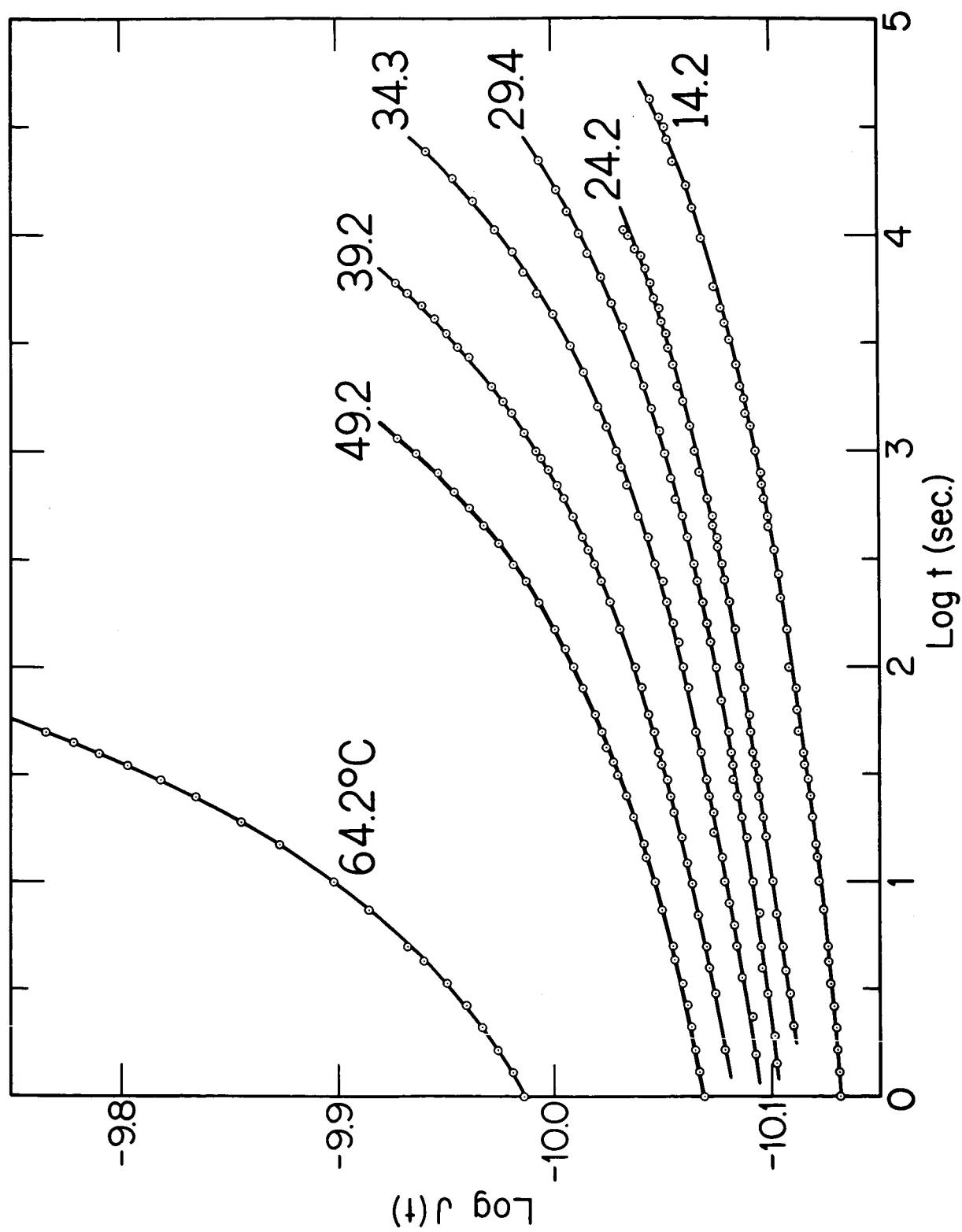


Figure 8

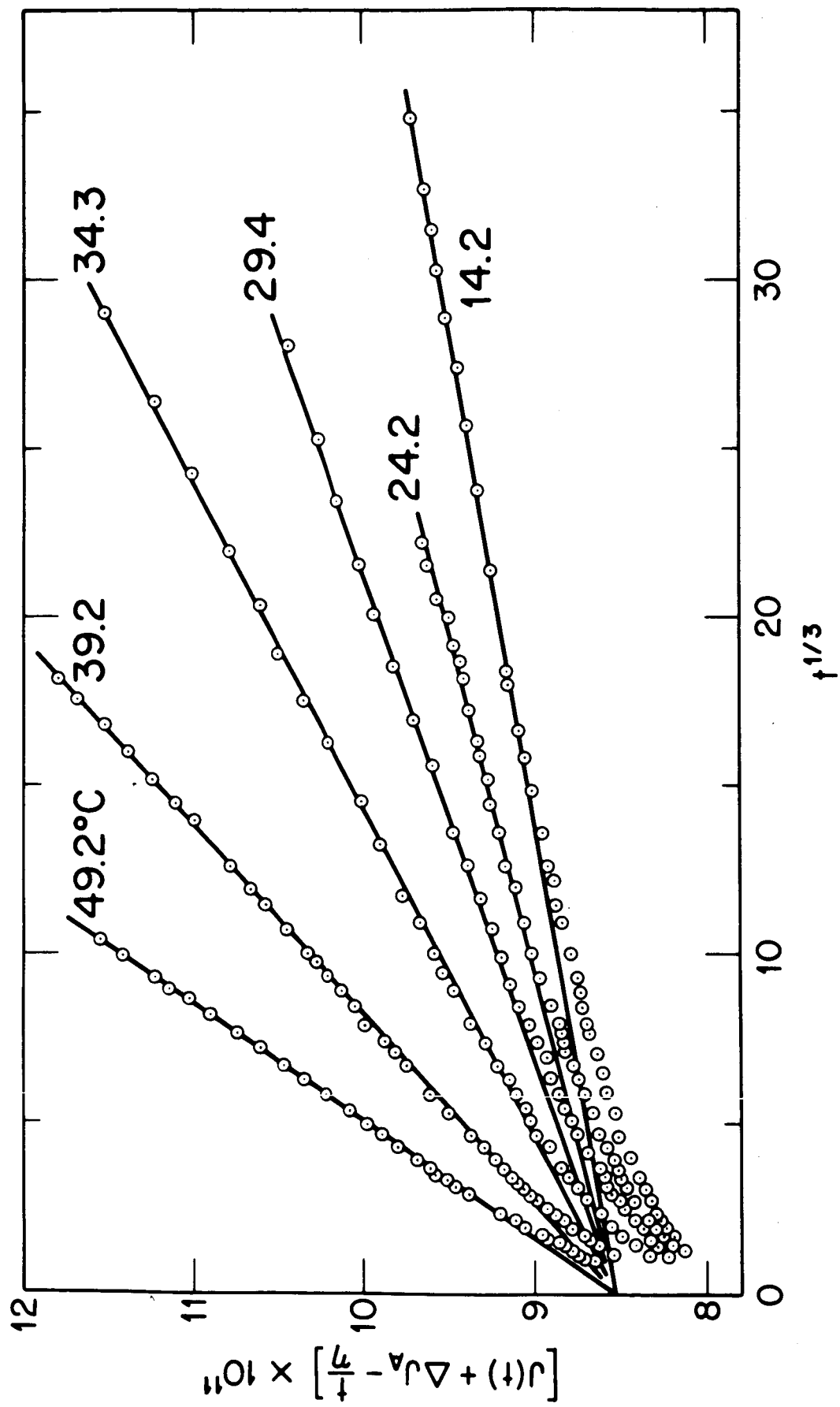


Figure 9

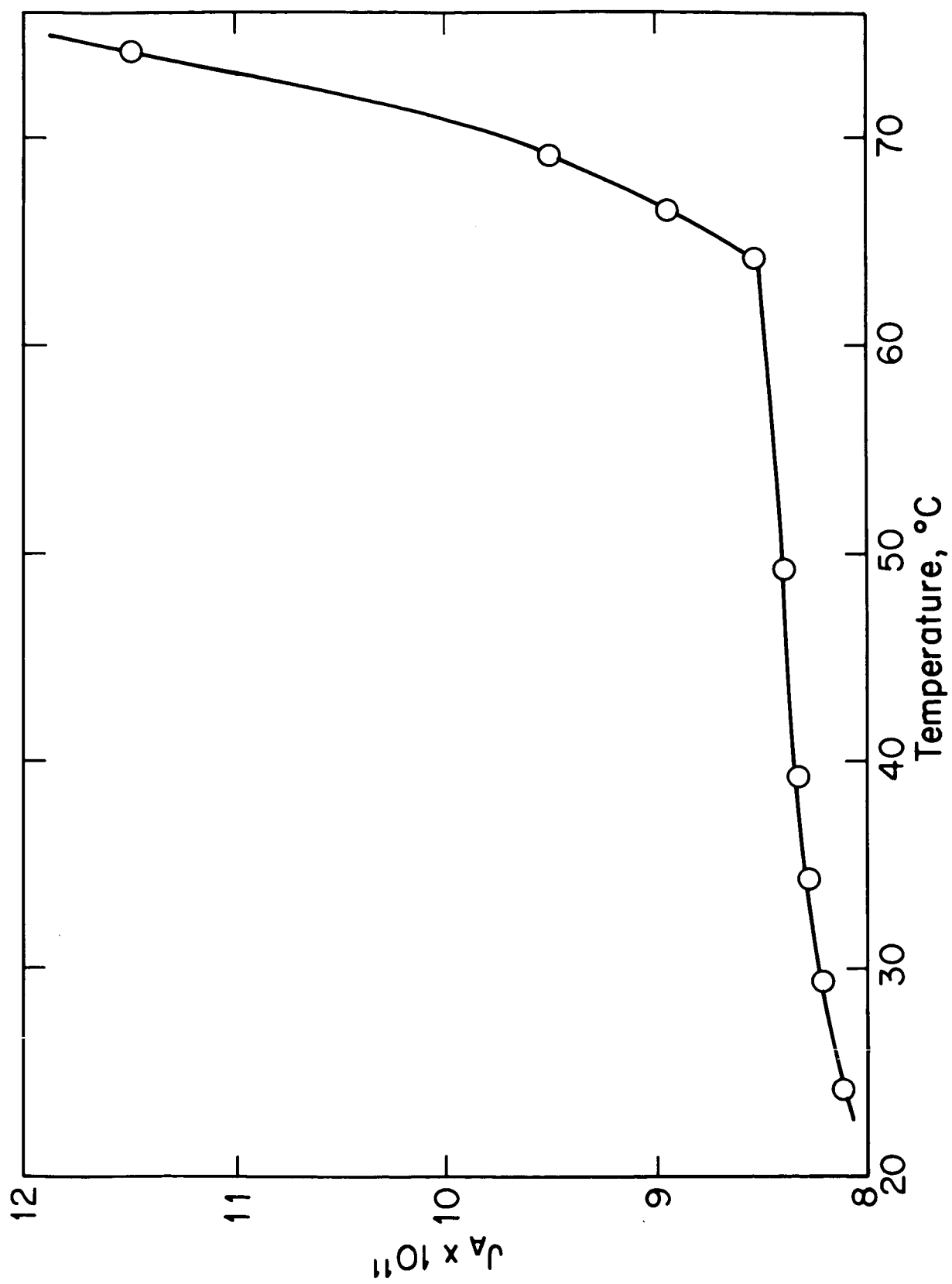


Figure 10

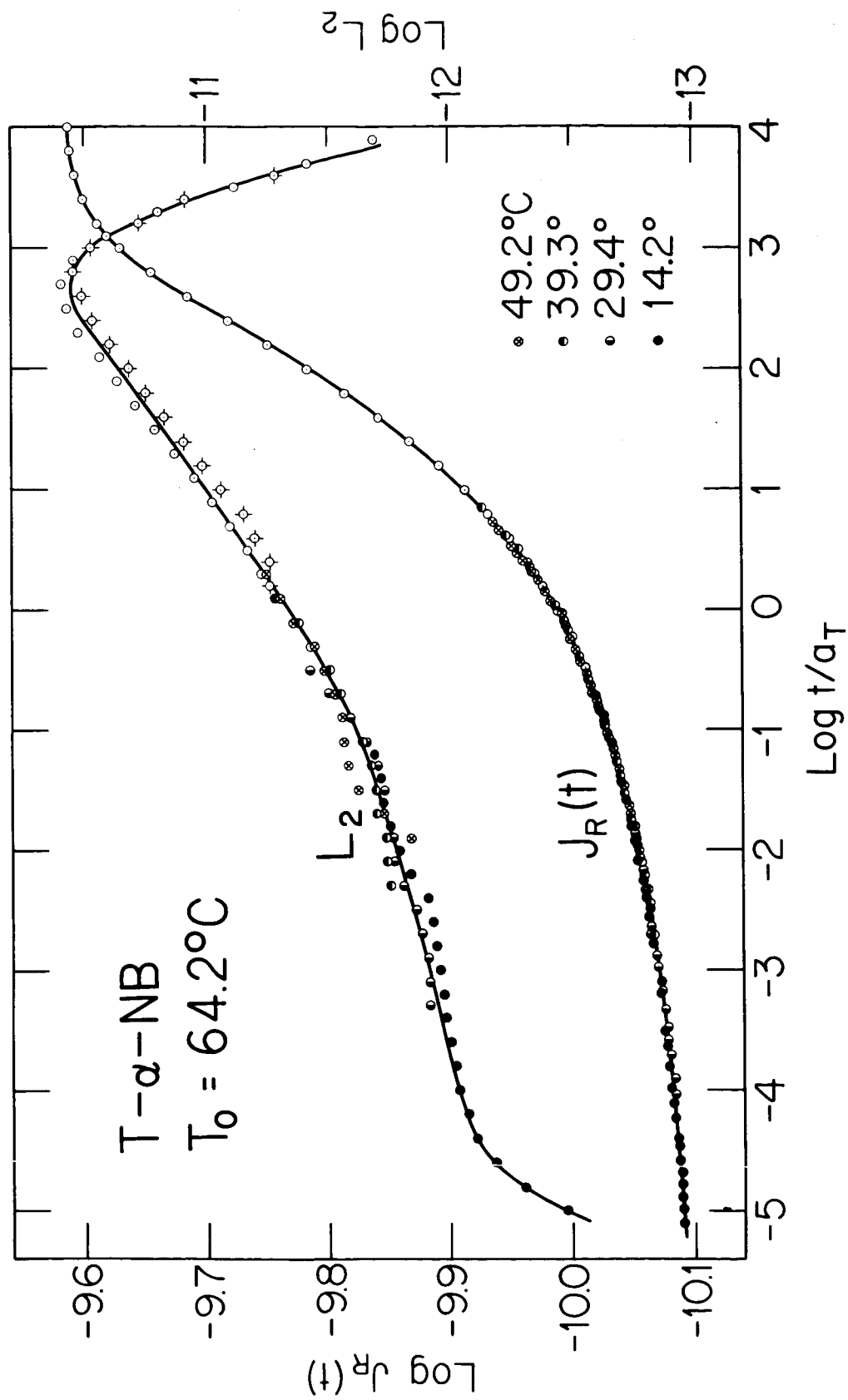


Figure 11

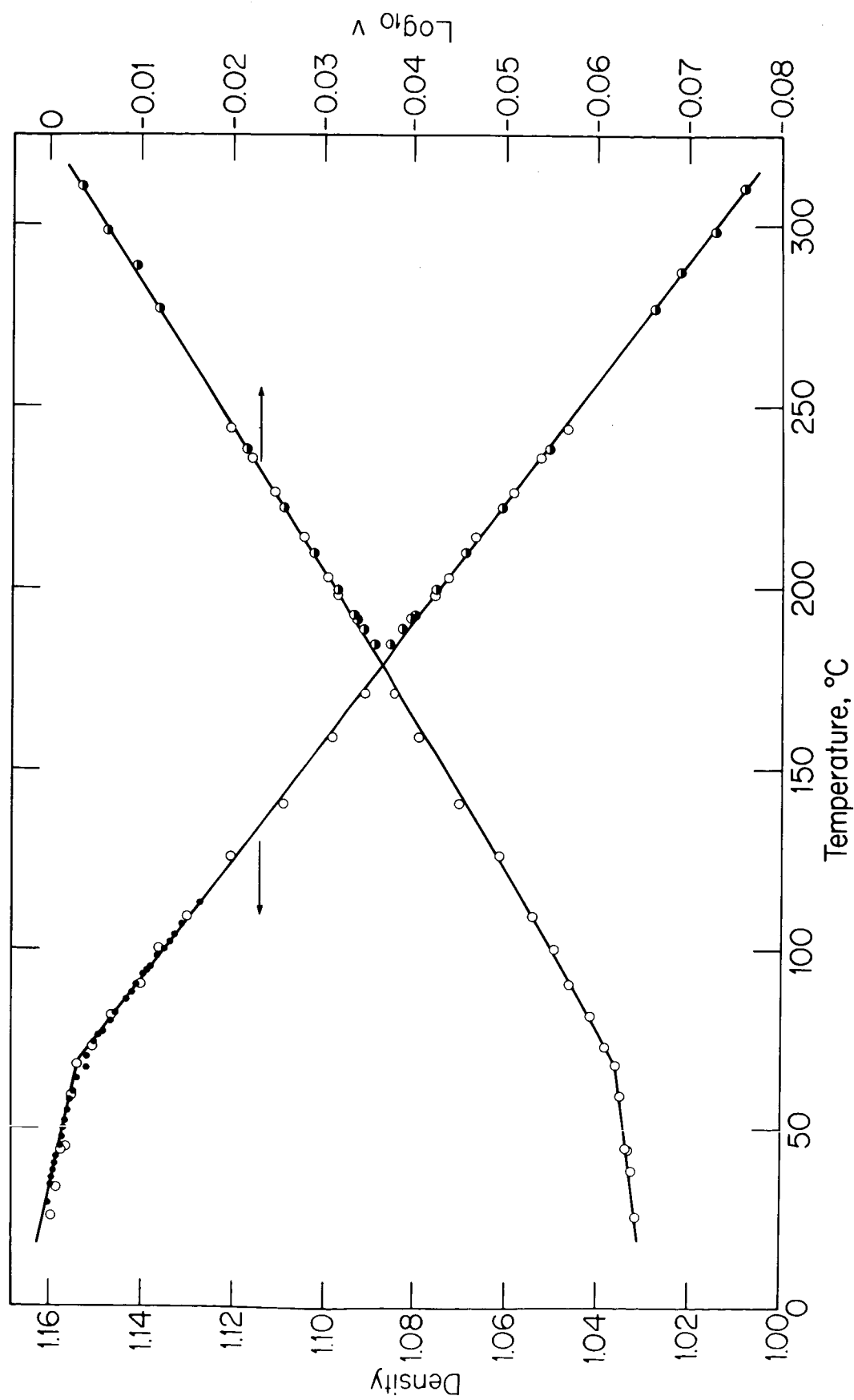


Figure 12

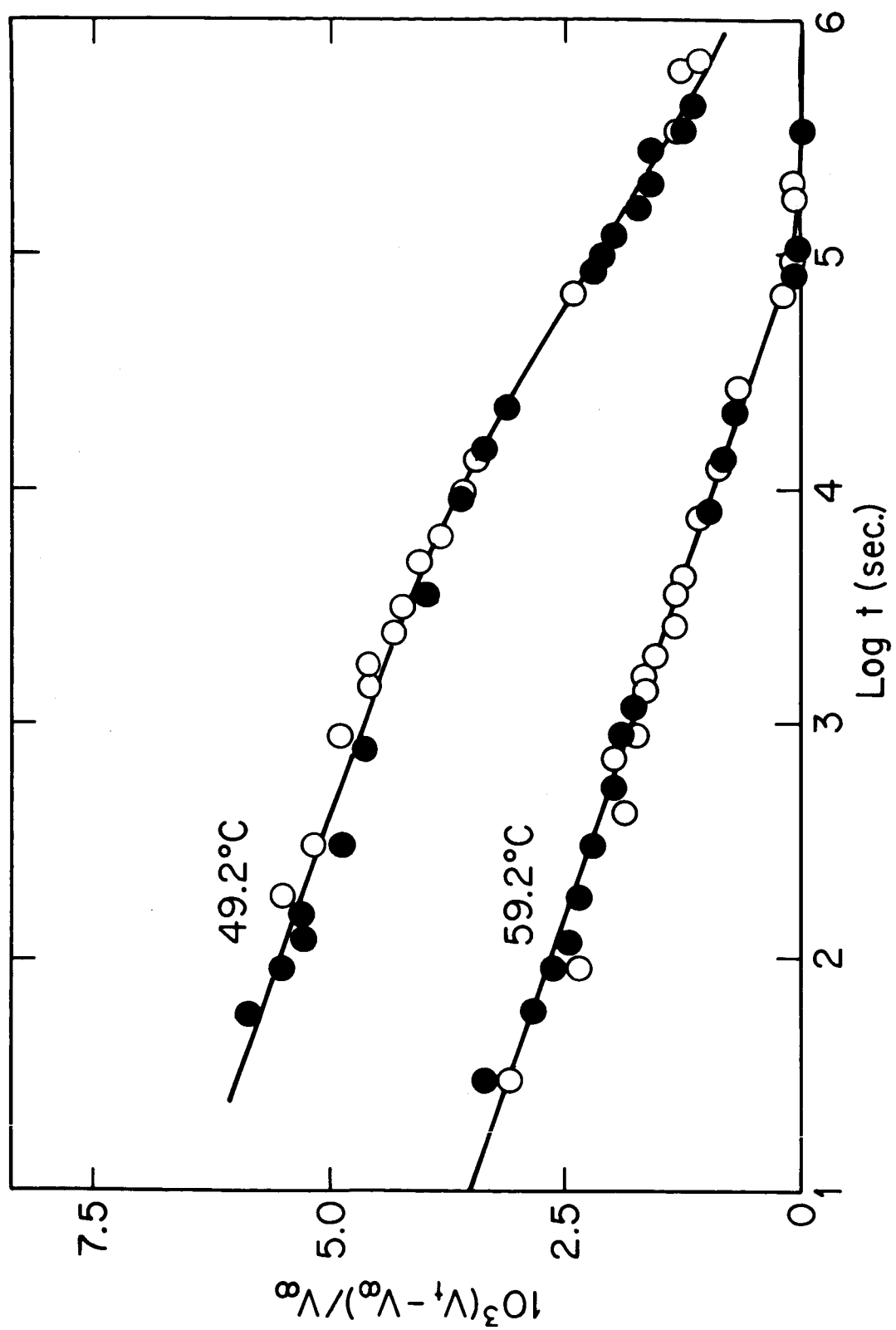


Figure 13

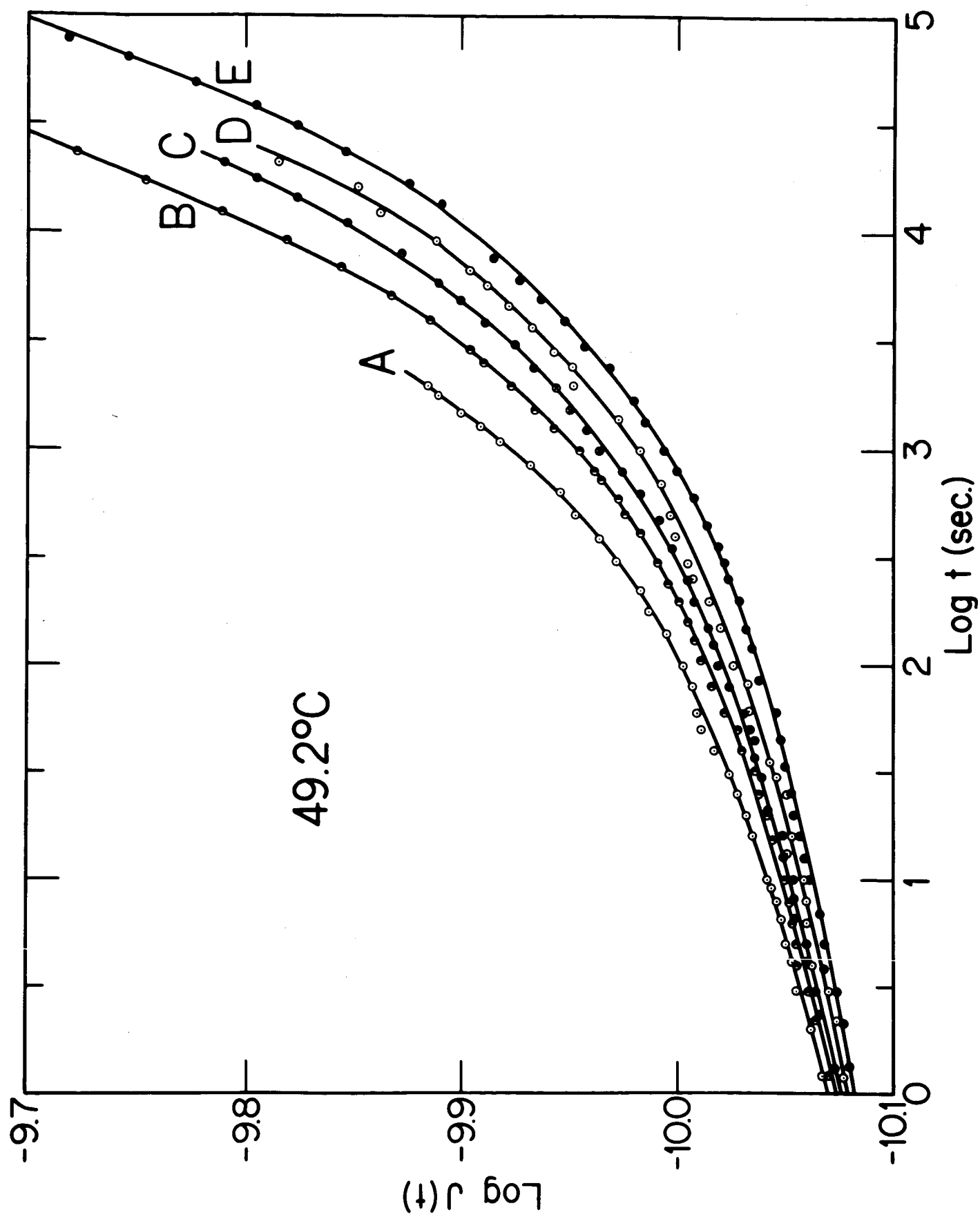


Figure 14

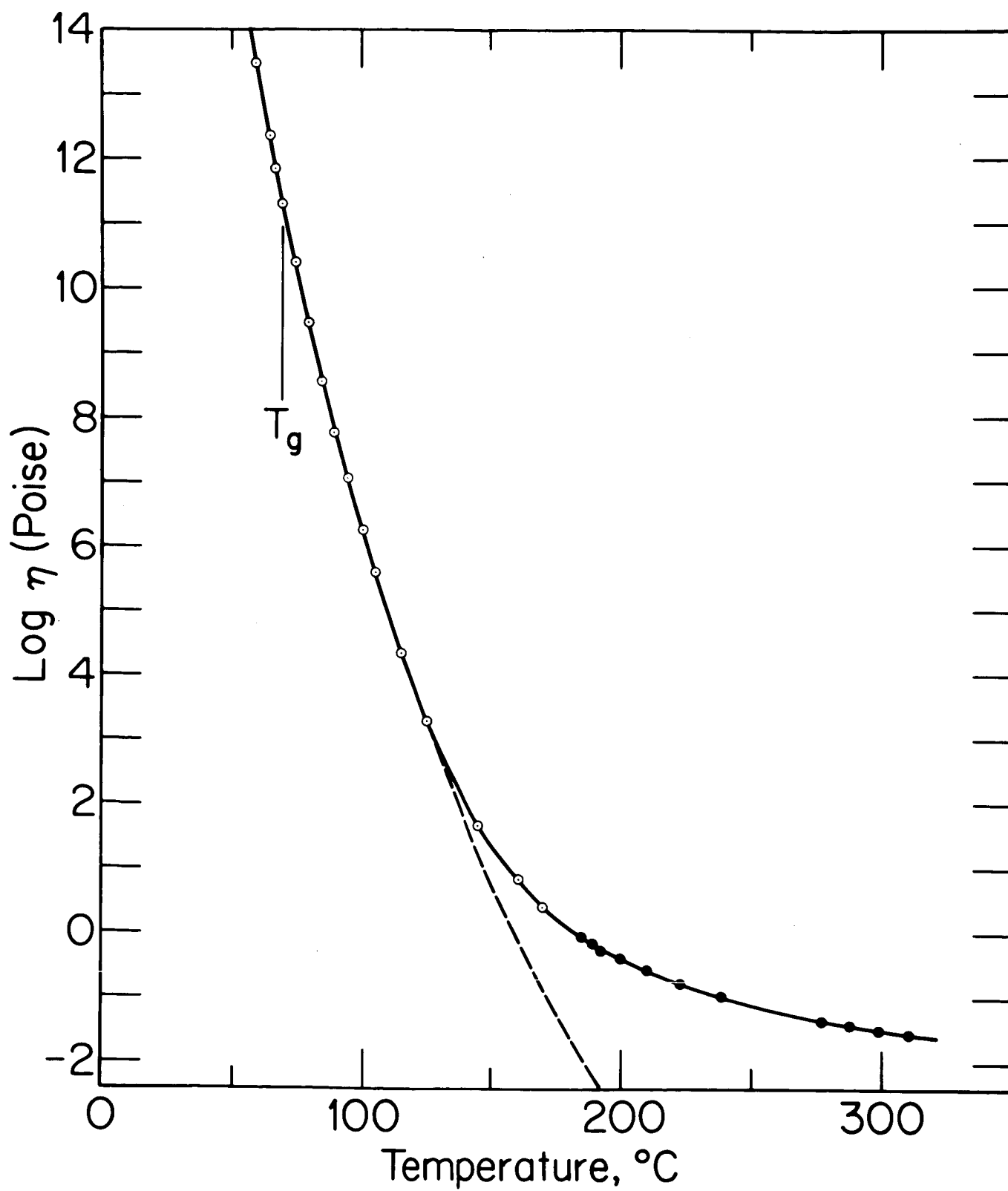


Figure 15

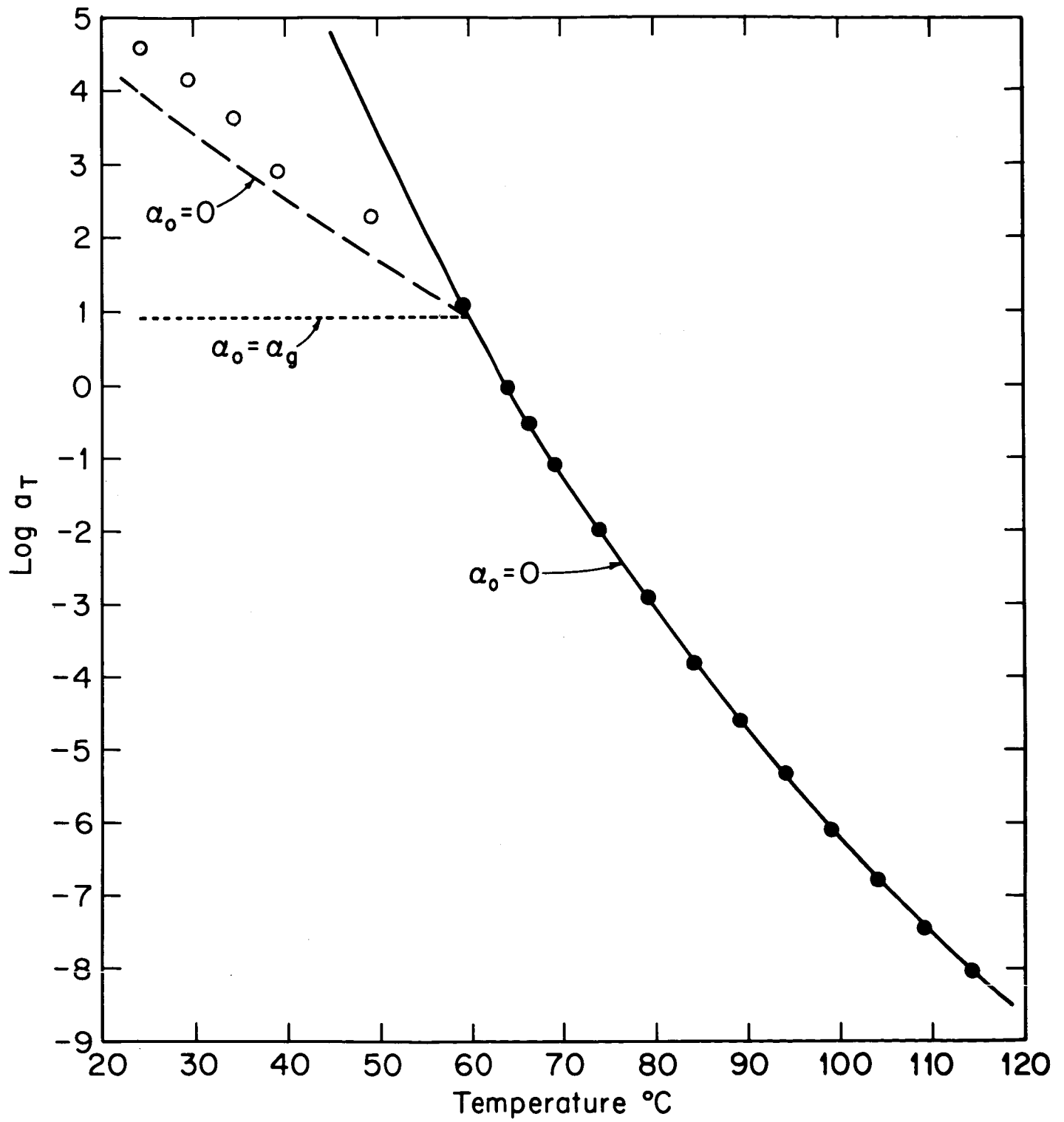


Figure 16

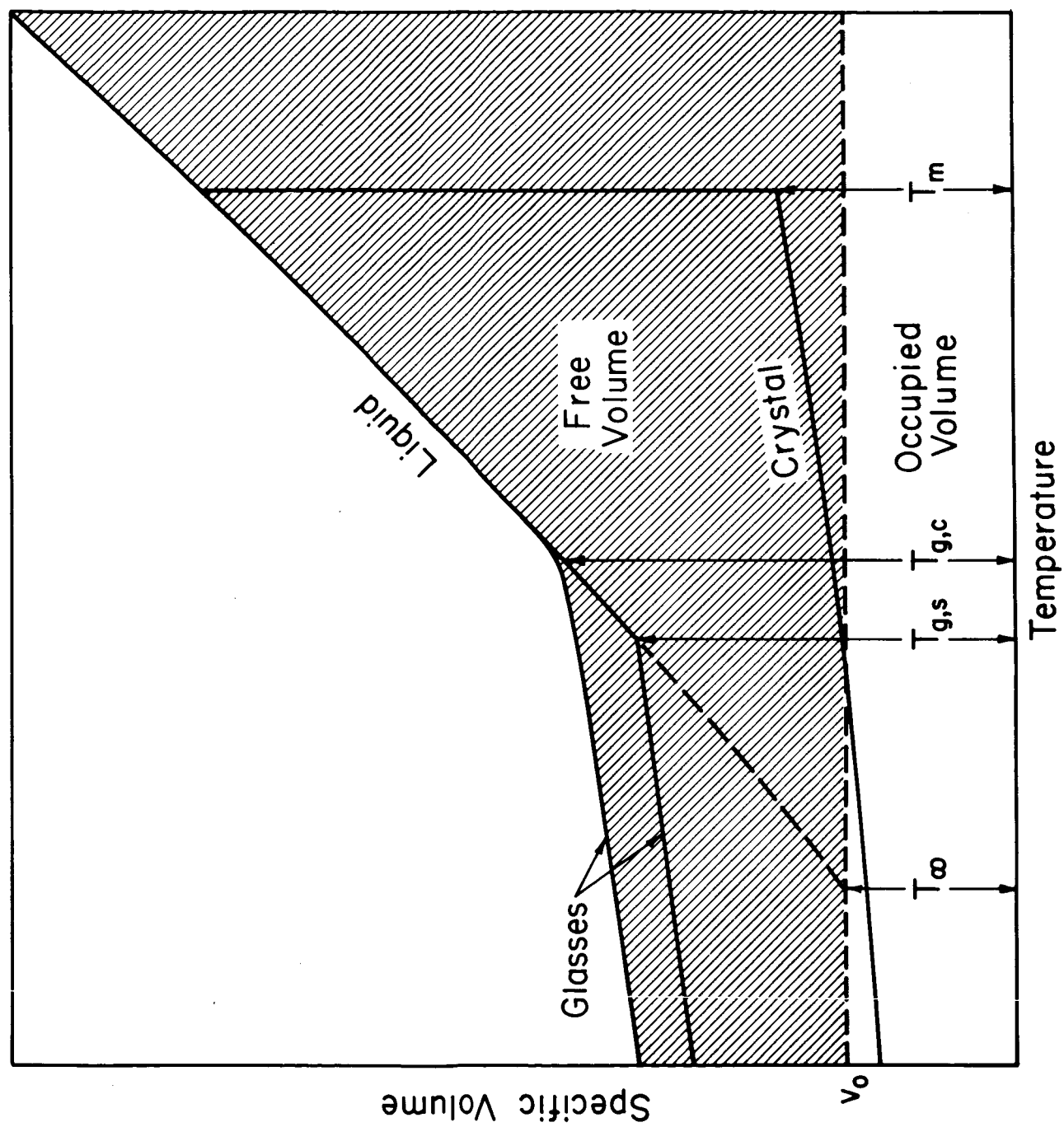


Figure 17

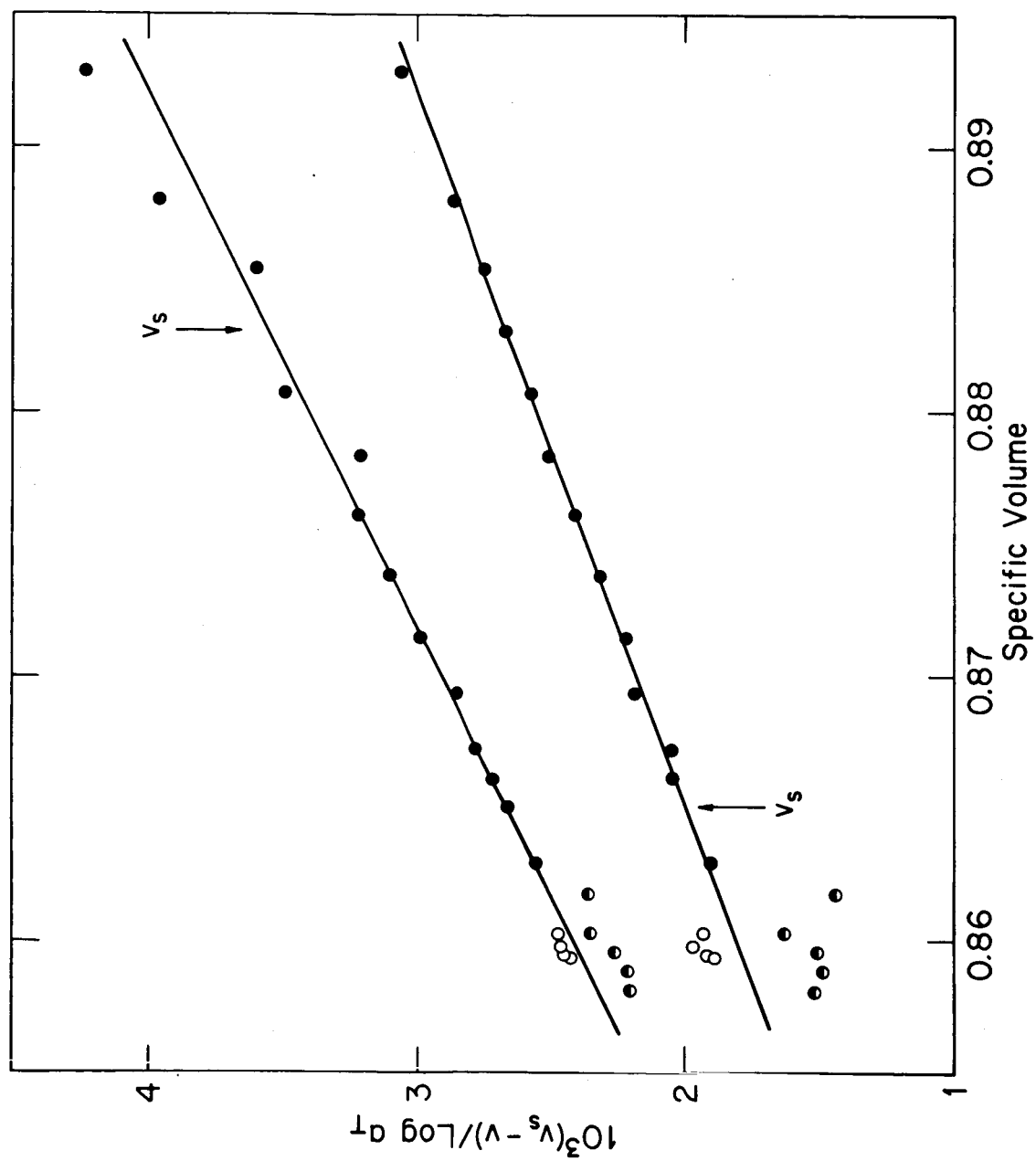


Figure 18